

# Accepted Manuscript

Pyrazole derived ultra-short antimicrobial peptidomimetics with potent anti-biofilm activity

Mija Ahn, Pethaiah Gunasekaran, Ganesan Rajasekaran, Eun Young Kim, Soo-Jae Lee, Guel Bang, Kun Cho, Jae-Kyung Hyun, Hyun-Ju Lee, Young Ho Jeon, Nam-Hyung Kim, Eun Kyoung Ryu, Song Yub Shin, Jeong Kyu Bang

PII: S0223-5234(16)30807-8

DOI: [10.1016/j.ejmech.2016.09.071](https://doi.org/10.1016/j.ejmech.2016.09.071)

Reference: EJMECH 8937

To appear in: *European Journal of Medicinal Chemistry*

Received Date: 2 August 2016

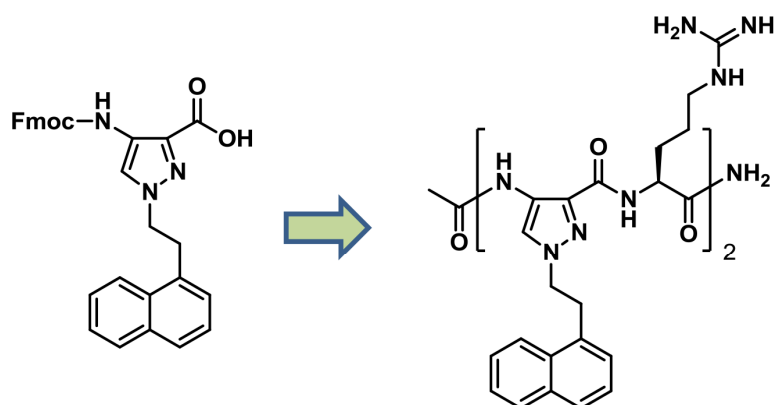
Revised Date: 20 September 2016

Accepted Date: 21 September 2016

Please cite this article as: M. Ahn, P. Gunasekaran, G. Rajasekaran, E.Y. Kim, S.-J. Lee, G. Bang, K. Cho, J.-K. Hyun, H.-J. Lee, Y.H. Jeon, N.-H. Kim, E.K. Ryu, S.Y. Shin, J.K. Bang, Pyrazole derived ultra-short antimicrobial peptidomimetics with potent anti-biofilm activity, *European Journal of Medicinal Chemistry* (2016), doi: 10.1016/j.ejmech.2016.09.071.

This is a PDF file of an unedited manuscript that has been accepted for publication. As a service to our customers we are providing this early version of the manuscript. The manuscript will undergo copyediting, typesetting, and review of the resulting proof before it is published in its final form. Please note that during the production process errors may be discovered which could affect the content, and all legal disclaimers that apply to the journal pertain.





- *Antimicrobial*
- *Anti-inflammatory*
- *Anti-biofilm Activity*
- *Anti-MRSA*
- *Anti-VREF*
- *Anti-MDRPA*
- *Proteolytic Stability*
- *Non-Cytotoxicity*

Fmoc-Pyrazole Amino Acid

Pyrazole derived Ultra-short Peptidomimetic

## Pyrazole Derived Ultra-short Antimicrobial Peptidomimetics with Potent Anti-biofilm Activity

Mija Ahn,<sup>1¶</sup> Pethaiah Gunasekaran,<sup>2¶</sup> Ganesan Rajasekaran,<sup>3¶</sup> Eun Young Kim,<sup>3¶</sup> Soo-Jae Lee,<sup>4</sup> Guel Bang,<sup>5</sup> Kun Cho,<sup>5</sup> Jae-Kyung Hyun,<sup>6</sup> Hyun-Ju Lee,<sup>6,7</sup> Young Ho Jeon,<sup>8</sup> Nam-Hyung Kim,<sup>2</sup> Eun Kyoung Ryu,<sup>1,9</sup> Song Yub Shin,<sup>3\*</sup> Jeong Kyu Bang<sup>1,9\*</sup>

<sup>1</sup>Division of Magnetic Resonance, Korea Basic Science Institute, Ochang, Chung-Buk 363-883, Republic of Korea, <sup>2</sup>Molecular Embryology Laboratory, Department of Animal Sciences, Chungbuk National University, Chung-Buk 361-763, Republic of Korea, <sup>3</sup>Department of Medical Science, Graduate School and Department of Cellular & Molecular Medicine, School of Medicine, Chosun University, Gwangju 501-759, Republic of Korea. <sup>4</sup>College of Pharmacy, Chungbuk National University, Chungbuk 361-763, Republic of Korea. <sup>5</sup>Biomedical Omics Group, Korea Basic Science Institute, Ochang, Chung-Buk 363-883, Republic of Korea, <sup>6</sup>Division of Electron Microscopic Research, Korea Basic Science Institute, 113 Gwahakro, Daejeon 305-333, <sup>7</sup>Department of Chemistry, Chungnam National University, Daejeon 305-764, Republic of Korea, <sup>8</sup>College of Pharmacy, Korea University, 2511 Sejong-Ro, Sejong, 30019, Republic of Korea, <sup>9</sup>Department of Bio-analytical Science, University of Science & Technology, Daejeon 34113, Republic of Korea.

\*Corresponding authors:

Jeong Kyu Bang, Ph.D.

Korea Basic Science Institute

Ochang, Chungbuk 363-883, Cheongwon

Republic of Korea

Tel: +82-43-240-5023, Fax: +82-43-240-5059

E-mail: [bangjk@kbsi.re.kr](mailto:bangjk@kbsi.re.kr)

Song Yub Shin, Ph.D.

Dept. Cellular & Molecular Medicine,

School of Medicine, Chosun University

Gwangju 501-759, Republic of Korea

Tel: +82-62-230-6769, Fax: +82-62-233-6337

E-mail address: [syshin@chosun.ac.kr](mailto:syshin@chosun.ac.kr)

¶These authors contributed equally to this work.

**Abstract**

In this study, we report on the first chemical synthesis of ultra-short pyrazole-arginine based antimicrobial peptidomimetics derived from the newly synthesized *N*-alkyl/aryl pyrazole amino acids. Through the systematic tuning of hydrophobicity, charge, and peptide length, we identified the shortest peptide Py11 with the most potent antimicrobial activity. Py11 displayed greater antimicrobial activity against antibiotic-resistant bacteria, including MRSA, MDRPA, and VREF, which was approximately 2-4 times higher than that of melittin. Besides its higher selectivity (therapeutic index) toward bacterial cells than LL-37, Py11 showed highly increased proteolytic stability against trypsin digestion and maintained its antimicrobial activity in the presence of physiological salts. Interestingly, Py11 exhibited higher anti-biofilm activity against MDRPA compared to LL-37. The results from fluorescence spectroscopy and transmission electron microscopy (TEM) suggested that Py11 kills bacterial cells possibly by integrity disruption damaging the cell membrane, leading to the cytosol leakage and eventual cell lysis. Furthermore, Py11 displayed significant anti-inflammatory (endotoxin-neutralizing) activity by inhibiting LPS-induced production of nitric oxide (NO) and TNF- $\alpha$ . Collectively, our results suggest that Py11 may serve as a model compound for the design of antimicrobial and antiseptis agents.

**Keywords:** Ultra-short Peptidomimetics, Pyrazole-derived amino acids, Antimicrobial activity, Anti-biofilm activity, Bacterial killing mechanism

## 1. Introduction

In the past few decades, the discovery of new antibiotics has gained significant importance due to their prominent roles in treating diseases [1]. However, frequent, excessive and the widespread use of antibiotics results in the remarkable development of drug-resistant bacteria called as “superbugs” or “nightmare bacteria,” which are the challenging and severe threats to modern health care [2-5]. Thus, the emergence of multidrug-resistant (MDR) microbials and the dearth of new antibiotics led us to meet an urgent requirement for developing alternative and effective antimicrobial agents. Antimicrobial peptides (AMPs) have gained significant importance as host defense system in various creatures such as insects, plants, amphibians, and mammals [6-8]. In general, AMPs are oligopeptides containing excess positively charged and hydrophobic amino acids, which can adopt the amphipathic conformations upon contact with microbial membranes [9-13]. Usually, AMP killing mechanism of pathogens involves either (i) disruption of the membrane integrity by interacting with negatively charged membrane components, (ii) association with specific intracellular targets or (iii) inhibition of proteins, DNA and RNA synthesis [14]. Besides, AMPs have attracted significant interest as a new generation of antibiotics because of their broad-spectrum of antimicrobial activity against fungi, bacteria, and enveloped viruses at the physiological concentration. The distinctive mode of action and rapid killing rate of the AMPs result in the low propensity for developing resistance and enhance the efficacy for combating multi-drug resistance bacteria [15,16].

Although several AMPs possess promising merits as a novel tool to combat antibiotic-resistant pathogens, their pharmaceutical advancement into therapeutic agents is restricted by the intrinsic drawbacks such as large size, expensive production cost, susceptibility to protease degradation,

poor activity in the presence of salts and cytotoxicity to the host cells [17]. Moreover, the clinical use of AMPs sequences that are similar to the natural human AMPs may cause the inevitable loss of potential in the natural human defense [18]. To circumvent the hurdles limiting their applications, a few approaches have emerged including the *de novo* synthesis of peptides or modification in sequences of peptides, and the development of new peptidomimetics resembling the properties of AMPs. To develop new peptidomimetics, so far, several strategies have been adapted to synthesize the antimicrobial peptidomimetics including peptoids [19–22],  $\beta$ -peptides [23], aryl amide oligomers [24], oligourea [25],  $\beta$ -turn mimetics [26], and lipopeptides [27]. However, these moieties suffer from major disadvantages such as poor water solubility, complex synthetic routes, and difficulty in introducing various functional groups to achieve activity and unique selectivity.

To overcome the above limitations and to perform the effective structure-activity relationship (SAR), it is important to design the short and structurally simple peptidomimetics possessing unnatural amino acids with positive charge and hydrophobicity. Taking the above facts into the considerations, we have focused on developing the short and structurally simple peptidomimetics having unnatural amino acids. The present study stems as a part of our research program recently embarked on discovering the new and short peptidomimetics for antimicrobial studies [28–31].

In this work, we have designed and synthesized the peptidomimetics consisting of only two components, arginine (R) and *N*-alkyl/aryl pyrazoles (Py). The peptidomimetics were designed in the pattern of  $-(RPy)_n-$  repeating units, where R is responsible for the maintenance of positive charge [32], and the medically important pyrazole skeleton anchoring various alkyl or

aryls at the nitrogen(-NH) maintains the hydrophobicity [33]. To synthesize ultra-short AMPs, we have synthesized Fmoc-protected, *N*-substituted pyrazole amino acids for the first time, which have been used for straight forward solid phase peptide synthesis (SPPS) method to save the time and to maintain the structural diversity. These ultra-short peptidomimetics were examined for their antimicrobial activities against both Gram-positive and Gram-negative bacterial strains. The unnatural amino acid derived from pyrazole was expected to be more resistant to protease in *in vivo* as well as *in vitro* compare to the His modified AMPs that was reported by our group [29–31].

Among the designed peptidomimetics, Py11 displayed the most potent antimicrobial activity. Furthermore, it was evaluated for their antimicrobial activity against several antibiotic-resistant strains including methicillin-resistant *Staphylococcus aureus* (MRSA), multidrug-resistant *Pseudomonas aeruginosa* (MDRPA), and vancomycin-resistant *Enterococcus faecium* (VREF). In addition, cytotoxicity of Py11 against sheep red blood cells (sRBCs), RAW264.7 and NIH-3T3 cells was also investigated. The outer membrane (OM) permeability, inner membrane (IM) permeability, membrane depolarization, and transmission electron microscope (TEM) were studied extensively for understanding the bacterial killing mechanism. The antimicrobial activity in the presence of physiological salts and proteolytic stability to trypsin digestion of Py11 were also examined. Next, the ability of Py11 to inhibit the formation of bacterial biofilm against MDRPA was evaluated. Additionally, the anti-inflammatory (endotoxin-neutralizing) activity of Py11 by inhibiting LPS-induced production of nitric oxide (NO) and tumor necrosis factor- $\alpha$  (TNF- $\alpha$ ) was investigated.

## 2. Results and Discussion

### 2.1 Synthesis of pyrazole-derived amino acids and peptidomimetics

In search of discovering unique scaffold for developing ultra-short antimicrobial peptidomimetics, we have identified the *N*-alkyl/aryl pyrazole derivatives as a key skeleton backbone for structural and biological properties of AMPs (Scheme 1). The commercially available 4-nitro-3-pyrazolecarboxylic acid was used as a starting material for the synthesis of Fmoc-protected pyrazole amino acid derivatives. Initially, the esterification of nitro-3-pyrazolecarboxylic acid was carried out using thionyl chloride and methanol under reflux condition to yield **1**. Then, the *N*-alkylation of **1** was achieved using various alkyl or aryl halides in the presence of potassium carbonate in DMF to yield **2**. The Pd/C reduction of nitro group resulted in the formation of amine, and subsequent Fmoc protection using Fmoc-Osu in the presence of sodium bicarbonate yielded the Fmoc protected amine (**3**). Finally, lithium iodide mediated methyl ester hydrolysis resulted in the formation of desired Fmoc-protected, *N*-alkyl/aryl pyrazole amino acid derivatives, **4** in good yields. The synthesized Fmoc-protected pyrazole amino acids were successfully adopted for the generation of peptide library using Rink amide resin by the conventional solid-phase peptide synthesis (Figure 1). To initiate the sequence extension, firstly Fmoc-Arg (pbf)-OH was added to the free amine on the resin to enable the amide coupling in the presence of HBTU, HOBt, and DIEA in DMF. After stirring for 1 h, the Fmoc deprotection was achieved by treating with 20% piperidine in DMF, and the next amino acid was coupled. This procedure has been repeated for other amino acids coupling until we get the desired peptidomimetics. Finally, the peptide cleavage from the resin was achieved by a mixture of trifluoroacetic acid, water, and triisopropylsilane (90:5:5, v/v/v, 2 mL). The peptides were purified using preparative RP-HPLC. The molecular weight of peptidomimetics was

determined by matrix-assisted laser-desorption ionization time-of-flight mass spectrometry (MALDI-TOF MS). The cyclic peptide was synthesized from the linear side-chain protected peptides. The Fmoc group in the linear peptides was deprotected using piperidine in DMF, and the *N*-terminal amine was bromoacetylated using of BrCH<sub>2</sub>COOH in the presence of DIC. Then the peptide was cleaved from the resin and treated with triethylamine until the solution turns into basic condition (pH 8-9). Under this condition, spontaneous intramolecular cyclization was taken place through the cysteine thiol addition over *N*-bromoacetyl group. Further purification through preparative RP- HPLC and MALDI-TOF-MS analysis confirmed the cyclization process.

## 2.2 Structure-antimicrobial activity study

The antimicrobial activities of newly synthesized peptidomimetics were screened against two Gram-negative bacteria (*Escherichia coli* [KCTC 1682] and *Pseudomonas aeruginosa* [KCTC 1637]) and two Gram-positive bacteria (*Staphylococcus epidermidis* [KCTC 1917] and *Staphylococcus aureus* [KCTC 1621]). Human cathelicidin LL-37 and bee venom melittin are used as positive control peptides for comparing their antimicrobial and hemolytic activities.

Initially, we started our antimicrobial screening studies for the newly synthesized dipeptide-Py1, which attached with *N*-2-ethylbutyl group at pyrazole. Unfortunately, the dipeptide did not show any considerable antimicrobial activity even at maximum concentration (64 µg/mL) (Table 1). To increase the charge, we introduced the Arg at the *N*-terminal position of the dipeptide-Py1, which resulted in the formation of Py2. This increase in charge also did not show any considerable effect on antimicrobial activity. In view of increasing the hydrophobicity, we synthesized the dipeptide, Py3 using propylphenyl anchoring pyrazole residue and further increment of charge was achieved by the *N*-terminal Arg addition to result in the formation of

Py4. However, Py3 and Py4 did not display any antimicrobial activity. The dipeptide Py5 was a modification of Py3 by introducing biphenyl residue at alkyl side chain for improving the hydrophobicity. Surprisingly, Py5 showed the appreciable antimicrobial activity towards Gram-negative bacteria, *P. aeruginosa*. Even though Py5 was made up of only two residues, their antimicrobial activity was comparable to LL-37. It is pertinent to note that the balance between charge density and hydrophobicity is one of the crucial factors to determine the antimicrobial activity [34]. To evaluate the effect of charge in Py5, an Arg residue was further added to the *N*-terminal position to yield Py6, which exhibited strong antimicrobial activity against both *P. aeruginosa* and *S. aureus*. Surprisingly, the activity of Py6 against *S. aureus* and *P. aeruginosa* was about 4-8 times higher than the LL-37. Similarly, while comparing mellitin, Py6 displayed 2-4 folds of enhanced activity against *S. aureus* and *P. aeruginosa*. From the above results, it was observed that the increase in hydrophobicity elevated the antimicrobial activity. Hence, to further modify the structure, the dipeptide Py7 was synthesized using the naphthyl attached pyrazole residues and the subsequent *N*-terminal addition of Arg to Py7 resulted in the tripeptide, Py8. In contrast, Py7 did not show any measurable antimicrobial activity against both the strains. However, the Py8 displayed the activity similar to LL-37 in the case of *S. aureus*. Structural diversity is a key factor for studying the broad spectrum of antimicrobial activities. Hence, to attain the structural diversity, we planned to synthesize the tetramer, hexamer, and cyclo-peptidomimetics. Initially, tetra-peptide, Py9 with biphenyl pyrazole residue was synthesized, which showed moderate activity against all the bacterial strains, in particular, in the case of *S. aureus*, it displayed better activity than LL-37 and mellitin. This encouraging result motivated us for the further extension of tetra peptidomimetics to hexamer Py10. However, it displayed the reduced activity compared to the corresponding tetramer, Py9. Afterward, tetramer,

Py11 was derived from the alternative arrangement of Arg and *N*-ethyl-naphthyl pyrazole residues. Interestingly, this tetramer showed the good activity against all strains range from 4~32 µg/mL. Concerning LL-37, Py11 displayed eight folds elevated activity against both *P. aeruginosa* and *S. aureus*. Similarly, Py11 exhibited four folds of increased activity against both *P. aeruginosa* and *S. aureus* compared to melittin. Py12 was derived from Py11 by the addition Arg residue to increase the charge. Surprisingly there were no changes in the antimicrobial activities compared to Py11, and it displayed the similar activity as Py11. However, a further increment of tetramer Py11 to hexamer Py13 lost its activity completely against all the strains except *S. aureus*. It was reported that the cyclization of the linear peptides enhances the activity and protease stability [35,36]. Hence, the cyclic peptide Py14 was synthesized from the Py9 through the thioether bridging. However, Py14 displayed a poor spectrum of antimicrobial activity compare to the linear peptide Py9. Collectively, the structure activity study infers that, firstly, the hydrophobic units and charge find the crucial role in determining antimicrobial activity. Secondly, the peptide length was essential in discovering efficient peptidomimetics possessing good antimicrobial activity. For instance, even though the dipeptide Py7 and the tripeptide Py8 did not show any antimicrobial activity, the tetrapeptides (Py9 and Py11) were impressive in displaying antimicrobial activity against all the strains. Thus, among the all synthesized peptidomimetics, tetrapeptide Py11 displayed the most potent antimicrobial activity against all the tested strains. Hence, Py11 was selected as a lead compound for further studies.

### 2.3 Cell selectivity and cytotoxicity against mammalian cells of short AMP Py11

In terms of analyzing the cell selectivity of Py11 towards bacterial cells, the hemolytic

activity against sRBCs of Py11 was measured in the range of 0.5~512  $\mu\text{g/mL}$  (Figure 2). Interestingly, like LL-37, Py11 produced less than 5% hemolysis even at the highest concentration of 512  $\mu\text{g/mL}$ , whereas melittin found to be relatively toxic that produced 20.9%, 52.4%, and 74.5% hemolysis at 16, 32, and 64  $\mu\text{g/mL}$ , respectively. In general, the therapeutic potential of antimicrobial agents is mainly based on the selective killing of bacterial cells without displaying significant cytotoxicity towards the mammalian cells. Cell selectivity of the peptides is expressed as therapeutic index (TI) = MHC/GM, where MHC is peptide concentration needed to reach 10% lysis of human red blood cells, while GM is expressed as the geometric mean of MICs against four bacterial cells. The therapeutic index (TI) indicates the relative safety of the drug and the capability of a drug candidate to differentiate any pathogen from the host cells. Thus, larger TI values indicate greater cell selectivity. To compare the cell selectivity, we chose LL-37 and melittin as the references. Interestingly, Py11 displayed significant cell selectivity (TI value: 53.9) compared to melittin (TI value: 0.5) (Table 2). Besides, Py11 was about 2-folds more selective towards bacteria cells than LL-37. To further look into the cytotoxicity of Py11 against other mammalian cells, the viability against mouse macrophage RAW264.7 and fibroblast NIH-3T3 cells was determined using MTT assay. Py11 was found to be nontoxic to RAW264.7 and NIH-3T3 cells up to 32  $\mu\text{g/mL}$ , and 64  $\mu\text{g/mL}$ , respectively (Figure 3).

#### *2.4 Antimicrobial activity against antibiotic-resistant bacteria of Py11*

In the recent years, severe infections caused by multidrug-resistant bacteria such as MRSA, MDRPA, and VREF are being a major challenge for conventional antibiotic treatments. Hence, there is an urgent necessity for the evolution of new antibiotics, which can act on drug-resistant bacteria. To probe the efficacy of short AMP Py11 against multidrug-resistant bacteria,

we screened antimicrobial activity against three MRSA strains (CCARM 3089, CCARM 3090, and CCARM 3095), two MDRPA strains (CCARM 2109, and CCARM 2095) and a VREF strain (ATCC 51559). Interestingly, Py11 exhibited excellent antimicrobial activity against all the strains compare to melittin (Table 3). For instance, Py11 displayed 2 to 4-folds of better anti-MRSA activity than melittin. In the case of MDRPA strains, Py11 showed 4-folds of efficient activity than melittin. Similarly, Py11 was found to disclose 2-folds of potent anti-VREF activity than melittin. This result indicates that Py11 may serve as a new class of antimicrobial agent against drug-resistant bacteria.

### 2.5 Protease stability

The poor proteolytic stability of AMPs is one of the major obstacles for their therapeutic advancement. In particular, trypsin-like proteases that present in the body are more selective towards the hydrolysis of C-terminal amide bonds of lysine and arginine. Since Py11 consists a couple of arginine residues, its proteolytic stability has been investigated by tryptic degradation. As shown in Figure 4, after the trypsin incubation for 24 h, our lead compound Py11 retained its antimicrobial activity against *E. coli* and *S. aureus*, while melittin completely lost their antimicrobial activity due to the proteolytic degradation by trypsin.

### 2.6 Salt resistance

To examine whether the antimicrobial activity of Py11 was compromised in the presence of salts, we treated *E. coli* and *S. aureus* with different peptide concentrations under various salt conditions (physiological concentrations of 150 mM NaCl, 1 mM MgCl<sub>2</sub>, and 2.5 mM CaCl<sub>2</sub>).

As indicated in Table 4, Py11 maintained its strong activity against *E. coli* and *S. aureus* in the presence of different salts. This result suggests that the activity of Py11 might be particularly critical under physiological conditions or in the treatment of infections that disturb the normal salt homeostasis in certain human tissues.

### 2.7. Antibiofilm activity

The biophysical properties of the biofilm extend extreme antibiotic resistance to microorganisms [37]. The ability of the peptides to inhibit the formation of bacterial biofilm was evaluated against MDRPA (CCARM 2095). The potent inhibitory activity of LL-37 on biofilm formation of *Staphylococcus epidermidis* and *Pseudomonas aeruginosa* has been reported [38,39]. Therefore, we used LL-37 as a reference AMP to compare the antibiofilm activity with Py11. The IC<sub>90</sub> (the concentration of the compounds that inhibits 90% biofilm development) values of Py11 and LL-37 against MDRPA biofilm formation was 16 µg/mL, and 64 µg/mL, respectively (Figure 5). This result demonstrates that Py11 was potent enough to inhibit the MDRPA biofilm formation. Thus, the efficient antibiofilm activity of Py11 makes it promising anti-biofilm agents.

### 2.8 Outer membrane permeability

The ability of Py11 to permeate the outer membrane of Gram-negative bacteria was assessed by the fluorescent dye NPN uptake into the outer membrane of *E. coli*. The hydrophobic fluorescent probe NPN has a tendency to quench in an aqueous environment, in contrast, it exhibits strong fluorescence in the hydrophobic environment. Hence, there will be a substantial increase in fluorescence, when the dye enters the damaged membrane through the

destabilization of the bacterial outer membranes. We evaluated the NPN uptake assay using Py11 in a dose-dependent manner, and the results reveal that Py11 showed enhanced fluorescence intensity than the standards (Figure 6(A)). However, it obeys the fluorescence pattern as similar as melittin in a concentration-dependent manner, which implies that Py11 may follow the cell permeability mechanism similar to melittin.

### *2.9 Inner membrane permeability*

The inner membrane permeability of short AMP Py11 was evaluated by spectrophotometrically at 415 nm using ONPG hydrolysis method. The inner membrane permeability is measured by the bulk entry of nonchromogenic substrate ONPG, which undergoes subsequent cleavage to the yellow product ONP by the cytoplasmic  $\beta$ -galactosidase. To evaluate the inner membrane permeability, as shown in Figure 6(B), our lead peptide Py11 was experimented in a concentration-dependent manner. It is evident from the figure that Py11 demonstrated a significant ability to permeate the inner membrane as indicated by the greater slope of ONPG hydrolysis. Here, buforin-2 was used as a negative control due to the weak or poor inner membrane permeation even at higher concentrations, whereas melittin showed enhanced permeability compare to LL-37 as illustrated in Figure 6(B). It is evident from the above results that peptide Py11 displayed significant inner membrane permeability, and it followed an inner membrane permeable pattern like melittin.

### *2.10 Cytoplasmic membrane depolarization*

To evaluate the action of Py11 on the bacterial cytoplasmic membrane depolarization, we investigated the ability of our short peptide Py11 to depolarize the bacterial cytoplasmic membrane using a diSC<sub>3-5</sub>, which is a membrane potential-dependent probe. The dye diSC<sub>3-5</sub> was dispersed between the cells and medium, based on the cytoplasmic membrane potential, and it gets self-quenched when concentrated inside bacterial cells. During the membrane depolarization, there will be an increase in fluorescence intensity due to the dispersion of probe into the medium. Here, we used melittin and LL-37 as membrane-targeting AMP, and buforin-2 was used as intracellular-target AMP. Like melittin and LL-37, the addition of Py11 triggered a significant increase in fluorescence intensity indicating the rapid membrane depolarization (Figure 7). This result demonstrated that Py11 effectively induced a loss of membrane potential. In contrast, buforin-2 did not induce membrane depolarization.

### 2.11 Transmission electron microscopy (TEM)

To envision the morphological changes in the *E. coli* and *S. aureus* caused by the action of Py11, transmission electron microscopy (TEM) images were recorded for the incubated mixtures of Py11 with *E. coli* and *S. aureus*. It was evident from Figure 8-A and 8-C that the untreated positive controls, *E. coli*, and *S. aureus*, possessed well-defined cell morphology. In contrast, the synthetic peptide Py11 treated cells from Figure 8-B and 8-D, showed the massive changes in the cellular structure with disruption in the bacterial cell membrane. These damages in cell membrane led to the formation of lysed cells with the release of cell content. Hence, it is evident from the above images that Py11 followed the cell membrane targeting mechanism of action against the bacterial cells.

### 2.12 Anti-inflammatory (endotoxin-neutralizing) activity

The outer membrane of Gram-negative bacteria contains lipopolysaccharide(LPS, endotoxin) as one of the main constituents. The release of LPS from bacteria into the bloodstream during infection may cause serious unwanted stimulation of host's immune system, leading to sepsis and septic shock of the patient [40,41]. In addition to their antimicrobial activity, some AMPs have been known to show potent anti-inflammatory (endotoxin-neutralizing) ability to suppress harmful inflammatory/septic responses [42–47]. These anti-inflammatory properties make AMPs attractive drug candidates for Gram-negative induced endotoxic shock and sepsis treatments. NO and TNF- $\alpha$  are the two important inflammatory products that are mainly associated in promoting the inflammatory response. Therefore, we examined the anti-inflammatory effect of Py11 using NO production and TNF- $\alpha$  release in LPS-stimulated RAW264.7 cells. NO release was determined by the Griess method to detect nitrite (NO<sub>2</sub><sup>-</sup>) accumulation in a cultured medium. The tnf- $\alpha$  release was determined by the commercial mouse ELISA kit. As shown in Figure 9, Py11 inhibited significantly NO and TNF- $\alpha$  release by LPS-stimulated macrophages in a concentration-dependent manner. Py11 inhibited more than 85% of the nitrite production at the peptide concentration of 16  $\mu$ g/mL. Similarly, it blocked more than 50% of TNF- $\alpha$  release at 32  $\mu$ g/mL. LPS induces the mRNA expression of iNOS and TNF- $\alpha$  in RAW264.7 cells, which correlates with NO and TNF- $\alpha$  release. Therefore, the effects of the peptides on LPS-induced the mRNA expression of inducible nitric oxide synthase (iNOS) and TNF- $\alpha$  were examined by RT-PCR. Py11 efficiently suppressed the mRNA expression of iNOS and TNF- $\alpha$  at 16  $\mu$ g/mL (Figure 10). This result is in agreement with the observed inhibition of NO and TNF- $\alpha$  release in Figure 9, confirming that Py11 has potent anti-inflammatory activity.

### 3. Conclusion

In conclusion, this article demonstrates that the first time synthesis of short peptidomimetics comprising of Arg and *N*-alkyl/aryl pyrazoles (Py) residues with good antimicrobial and anti-inflammatory activities without hemolytic activity and cytotoxicity against mammalian cells. The easily derivable peptidomimetics led to performing the effective SAR studies by the systematic tuning of hydrophobicity, charge, and peptide length. Also, our peptidomimetic Py11 proved to be a very promising lead compound having anti-MRSA, anti-VREF and anti-MDRPA activities, anti-biofilm activity and salt resistance. In addition to antimicrobial nature, enhanced proteolytic stability also adds the additional merits for Py11 to develop as a new class of antimicrobial agent. The mechanism of action against the pathogens was elucidated using fluorescence spectroscopy, and TEM study. Our results revealed that our peptidomimetic Py11 kills bacterial cells possibly by integrity disruption damaging the cell membrane, leading to the cytosol leakage and eventual cell lysis. Collectively, our results suggest that Py11 has tremendous potential to evolve as a model compound for antimicrobial and antiseptic agent design.

### 4. Experimental section

#### 4.1. Chemistry

All materials were obtained from commercial chemical suppliers and used as obtained. Anhydrous organic solvents were purchased from Aldrich packaged under N<sub>2</sub> in sure/seal bottles and used directly. Thin layer chromatography (TLC) was performed on Merck TLC plates, silica

gel 60 F254. Column chromatography was carried out on Merck silica gel 60 (70-230 mesh or 230-400 mesh).  $^1\text{H}$  and  $^{13}\text{C}$  NMR spectra were recorded on a Bruker DRX-400 spectrometer at 400 and 100 MHz, respectively. Chemical shifts ( $\delta$ ) are reported in parts per million (ppm) measured relative to an internal standard and coupling constants ( $J$ ) are expressed in hertz (Hz). Mass spectra were recorded using Shimadzu (MALDI-TOF) mass spectrometer. Lipopolysaccharide (LPS, from *Escherichia coli* O111:B4), Triton X-100, *N*-phenyl-1-naphthylamine (NPN), colorimetric 3-(4,5-dimethyl thiazol-2-yl)-2,5-diphenyltetrazolium bromide (MTT) dye, gramicidin D (GD), *O*-nitrophenyl- $\beta$ -D-galactopyranoside (ONPG), and sheep red blood cells (s-RBCs) were purchased from Sigma–Aldrich Co. (St. Louis, MO, USA). 3,3'-Dipropylthiadicarbocyanine iodide (diSC<sub>3-5</sub>) was obtained from Molecular Probes (Eugene, OR, USA). Dulbecco's modified eagle medium (DMEM) and fetal bovine serum (FBS) were supplied by HyClone (Seoul, Bioscience, Republic of Korea) and Lonza (Lonza Walkersville Inc., MD, USA), respectively. *E. coli* ML-35, a lactose, permease-deficient strain with constitutive cytoplasmic  $\beta$ -galactosidase activity (*lacI lacZ<sup>+</sup> lacY*), utilized for inner membrane permeability assays, was kindly provided by Prof. J. I. Kim (Gwangju Institute of Science and Technology, Korea). The ELISA kit for TNF- $\alpha$  was obtained from R&D Systems (Minneapolis, MN, USA). All other reagents were of analytical grade. Buffers were prepared using Milli-Q ultrapure water. All other reagents were of analytical grade.

#### 4.2. Synthesis of 4-Nitro-1H-pyrazole-3-carboxylic acid methyl ester (**1**)

To a solution of 4-nitro-3-pyrazolecarboxylic acid (3.14 g, 20.0 mmol) in MeOH (50 mL) was slowly added thionyl chloride (7.3 mL, 0.1 mol) at 0 °C. After the completion of the addition,

the temperature of the reaction mixture increased to 70 °C and stirred for 5 h. Methanol was removed in vacuo, and the resulting residue was poured into ice water and extracted with EtOAc. The organic layer was washed with 10 % NaHCO<sub>3</sub> solution, brine and dried over Na<sub>2</sub>SO<sub>4</sub>. The resulting reaction mixture concentrated in vacuo to afford **1** as a white solid (3.37 g, 99%). <sup>1</sup>H NMR (400 MHz, DMSO-*d*<sub>6</sub>) δ 8.93 (s, 1H), 3.89 (s, 3H); <sup>13</sup>C NMR (100 MHz, DMSO-*d*<sub>6</sub>) δ 161.4, 138.0, 133.7, 132.0, 53.3.

#### 4.3. General Procedure A for the synthesis of compound 2a-2d

##### 4.3.1. 1-(2-Ethylbutyl)-4-nitro-1H-pyrazole-3-carboxylic acid methyl ester (**2a**)

To a solution of **1** (1.0 g, 5.84 mmol) in DMF (20 mL) were added K<sub>2</sub>CO<sub>3</sub> (4.04 g, 29.2 mmol) and 1-bromo-2-ethylbutane (891 μL, 6.42 mmol). The reaction mixture was heated to 60 °C and stirred for 15 h. The reaction mixture was diluted with water and extracted with EtOAc. The organic layer was washed with water and brine, dried over MgSO<sub>4</sub>, and concentrated in vacuo. The crude product was purified by silica gel column chromatography (hexane-EtOAc, 3:1) to afford **2a** as a colorless oil (730 mg, 49%). <sup>1</sup>H NMR (400 MHz, CDCl<sub>3</sub>) δ 8.12 (s, 1H), 4.10 (d, *J* = 7.2 Hz, 2H), 4.00 (s, 3H), 1.93 (m, 1H), 1.40-1.28 (m, 4H), 0.93 (t, *J* = 7.5 Hz, 6H); <sup>13</sup>C NMR (100 MHz, CDCl<sub>3</sub>) δ 160.5, 138.2, 134.0, 130.5, 57.1, 53.1, 41.1, 22.9, 10.3; HRMS *m/z* calcd for C<sub>11</sub>H<sub>18</sub>N<sub>3</sub>O<sub>4</sub> (M+H)<sup>+</sup> 256.1297, found 256.1298.

##### 4.3.2. 4-Nitro-1-(3-phenylpropyl)-1H-pyrazole-3-carboxylic acid methyl ester (**2b**)

Compound **2b** was prepared from compound **1** and 3-phenylpropyl bromide following the general procedure A (white solid, 66%). <sup>1</sup>H NMR (400 MHz, CDCl<sub>3</sub>) δ 8.10 (s, 1H), 7.33-7.28 (m, 2H), 7.24-7.16 (m, 3H), 4.19 (t, *J* = 7.2 Hz, 2H), 3.99 (s, 3H), 2.69 (t, *J* = 7.4 Hz, 2H),

2.29 (m, 2H);  $^{13}\text{C}$  NMR (100 MHz,  $\text{CDCl}_3$ )  $\delta$  160.5, 139.7, 138.3, 134.1, 130.2, 128.7, 128.3, 126.5, 53.2, 53.1, 32.4, 30.8; HRMS  $m/z$  calcd for  $\text{C}_{14}\text{H}_{16}\text{N}_3\text{O}_4$  ( $\text{M}+\text{H}$ ) $^+$  290.1141, found 290.1141.

#### 4.3.3. 1-(3,3-Diphenyl)-4-nitro-1H-pyrazole-3-carboxylic acid methyl ester (**2c**)

Compound **2c** was prepared from compound **1** and 3,3-diphenylpropyl bromide following the general procedure A (white solid, 67%).  $^1\text{H}$  NMR (400 MHz,  $\text{CDCl}_3$ )  $\delta$  7.94 (s, 1H), 7.35-7.22 (m, 10H), 4.16 (t,  $J = 7.1$  Hz, 2H), 4.01 (s, 3H), 3.90 (t,  $J = 7.6$  Hz, 1H), 2.73 (m, 2H);  $^{13}\text{C}$  NMR (100 MHz,  $\text{CDCl}_3$ )  $\delta$  160.5, 142.8, 138.5, 130.4, 128.9, 127.6, 126.9, 53.2, 52.5, 48.4, 35.0; HRMS  $m/z$  calcd for  $\text{C}_{20}\text{H}_{20}\text{N}_3\text{O}_4$  ( $\text{M}+\text{H}$ ) $^+$  366.1454, found 366.1454.

#### 4.3.4. 1-[1-(2-Naphthalene-1-yl)ethyl]-4-nitro-1H-pyrazole-3-carboxylic acid methyl ester (**2d**)

Compound **2d** was prepared from compound **1** and 1-(2-bromoethyl)naphthalene following the general procedure A (white solid, 59%).  $^1\text{H}$  NMR (400 MHz,  $\text{CDCl}_3$ )  $\delta$  7.92-7.88 (m, 2H), 7.79 (d,  $J = 8.2$  Hz, 1H), 7.64 (s, 1H), 7.57-7.50 (m, 2H), 7.36 (m, 1H), 7.14 (d,  $J = 6.9$  Hz, 1H), 4.52 (t,  $J = 7.0$  Hz, 2H), 4.01 (s, 3H), 3.67 (t,  $J = 7.0$  Hz, 2H);  $^{13}\text{C}$  NMR (100 MHz,  $\text{CDCl}_3$ )  $\delta$  160.5, 138.6, 134.0, 133.9, 132.2, 131.3, 130.4, 129.2, 128.3, 127.2, 126.7, 126.0, 125.5, 122.6, 54.5, 53.2, 33.3; HRMS  $m/z$  calcd for  $\text{C}_{17}\text{H}_{16}\text{N}_3\text{O}_4$  ( $\text{M}+\text{H}$ ) $^+$  326.1141, found 326.1141.

### 4.4 General Procedure B for the synthesis of compound 3a-3d

4.4.1. 4-[(9-Fluoren-9-ylmethoxy)carbonylamino]-1-(2-ethylbutyl)-1H-pyrazole-3-carboxylic acid methyl ester (**3a**)

To a solution of **2a** (1.05 g, 4.11 mmol) in MeOH-CH<sub>2</sub>Cl<sub>2</sub> (60 mL, 5:1) was added 5% palladium on carbon (200 mg), and the resulting mixture was stirred under an atmosphere of H<sub>2</sub> at room temperature for 3 h. The reaction mixture was filtered through Celite and the filtrate was concentrated. The crude product was used in the next reaction without further purification. To the crude amine and NaHCO<sub>3</sub> (1.03 g, 12.3 mmol) in THF-H<sub>2</sub>O (50 mL, 1:1) was added Fmoc-OSu (2.08 g, 6.17 mmol) at 0 °C. The resulting mixture was allowed to come to room temperature and stirred for 3 h. The reaction mixture was diluted with EtOAc and washed with water and brine, dried over Na<sub>2</sub>SO<sub>4</sub>, and concentrated in vacuo. The residue was purified by silica gel column chromatography (hexane-EtOAc, 3:1) to afford **3a** as a semisolid (1.33 g, 72%). <sup>1</sup>H NMR (400 MHz, CDCl<sub>3</sub>) δ 8.46 (s, 1H), 7.98 (s, 1H), 7.80 (d, *J* = 7.4 Hz, 2H), 7.65 (d, *J* = 7.4 Hz, 2H), 7.44 (t, *J* = 7.4 Hz, 2H), 7.36 (t, *J* = 7.4 Hz, 2H), 4.48 (d, *J* = 7.2 Hz, 2H), 4.31 (t, *J* = 7.2 Hz, 1H), 4.06 (d, *J* = 7.4 Hz, 2H), 4.01 (s, 3H), 1.93 (m, 1H), 1.38-1.28 (m, 4H), 0.90 (t, *J* = 7.4 Hz, 6H); <sup>13</sup>C NMR (100 MHz, CDCl<sub>3</sub>) δ 164.2, 153.3, 143.7, 141.3, 129.1, 127.8, 127.2, 125.9, 125.1, 120.9, 120.1, 67.7, 57.0, 52.1, 47.0, 41.5, 23.1, 10.5; HRMS *m/z* calcd for C<sub>26</sub>H<sub>30</sub>N<sub>3</sub>O<sub>4</sub> (M+H)<sup>+</sup> 448.2236, found 448.2236.

4.4.2. *4-[(9-Fluorenylmethoxy)carbonylamino]-1-(3-phenylpropyl)-1H-pyrazol-3-carboxylic acid methyl ester (3b)*

Compound **3b** was prepared from compound **2b** following the general procedure B (white solid, 67%). <sup>1</sup>H NMR (400 MHz, CDCl<sub>3</sub>) δ 8.45 (s, 1H), 8.00 (s, 1H), 7.80 (d, *J* = 7.4 Hz, 2H), 7.66 (d, *J* = 7.4 Hz, 2H), 7.44 (t, *J* = 7.4 Hz, 2H), 7.36 (t, *J* = 7.4 Hz, 2H), 7.33-7.18 (m, 5H), 4.50 (d, *J* = 7.2 Hz, 2H), 4.31 (t, *J* = 7.2 Hz, 1H), 4.18 (t, *J* = 7.2 Hz, 2H), 4.02 (s, 3H), 2.66 (t, *J* = 7.4 Hz, 2H), 2.26 (m, 2H); <sup>13</sup>C NMR (100 MHz, CDCl<sub>3</sub>) δ 164.2, 153.3, 143.7, 141.3,

140.4, 129.3, 128.6, 128.4, 127.9, 127.2, 126.3, 126.0, 125.1, 120.5, 120.1, 67.7, 53.0, 52.1, 47.0, 32.7, 31.7; HRMS  $m/z$  calcd for  $C_{29}H_{28}N_3O_4$  (M+H)<sup>+</sup> 482.2080, found 482.2081.

*4.4.3.4-[(9-Fluoren-9-ylmethoxy)carbonylamino]-1-(3,3-phenylpropyl)-1H-pyrazol-3-carboxylic acid methyl ester (3c)*

Compound **3c** was prepared from compound **2c** following the general procedure B (white solid, 70%). <sup>1</sup>H NMR (400 MHz, CDCl<sub>3</sub>) δ 8.40 (s, 1H), 7.89 (s, 1H), 7.78 (d,  $J = 7.4$  Hz, 2H), 7.63 (d,  $J = 7.4$  Hz, 2H), 7.42 (t,  $J = 7.4$  Hz, 2H), 7.35-7.17 (m, 12H), 4.47 (d,  $J = 7.2$  Hz, 2H), 4.28 (t,  $J = 7.2$  Hz, 1H), 4.09 (t,  $J = 7.3$  Hz, 2H), 3.98 (s, 3H), 3.90 (t,  $J = 7.9$  Hz, 1H), 2.66 (m, 2H); <sup>13</sup>C NMR (100 MHz, CDCl<sub>3</sub>) δ 164.1, 153.3, 143.7, 143.3, 141.3, 129.4, 128.8, 127.9, 127.7, 127.2, 126.7, 125.9, 125.1, 120.7, 120.1, 67.7, 52.2, 52.1, 48.4, 47.0, 35.9; HRMS  $m/z$  calcd for  $C_{35}H_{32}N_3O_4$  (M+H)<sup>+</sup> 558.2393, found 558.2394.

*4.4.4. 4-[(9-Fluoren-9-ylmethoxy)carbonylamino]-1-[2-(naphthalen-1-yl)ethyl]-1H-pyrazole-3-carboxylic acid methyl ester (3d)*

Compound **3d** was prepared from compound **2d** following the general procedure B (white solid, 76%). <sup>1</sup>H NMR (400 MHz, CDCl<sub>3</sub>) δ 8.45 (s, 1H), 8.06 (d,  $J = 8.2$  Hz, 1H), 7.93 (s, 1H), 7.90 (d,  $J = 8.2$  Hz, 1H), 7.82-7.79 (m, 3H), 7.66 (d,  $J = 7.2$  Hz, 2H), 7.60-7.51 (m, 2H), 7.47-7.35 (m, 5H), 7.30 (d,  $J = 7.2$  Hz, 1H), 4.52 (t,  $J = 7.6$  Hz, 2H), 4.49 (d,  $J = 7.1$  Hz, 2H), 4.31 (t,  $J = 7.1$  Hz, 1H), 4.05 (s, 3H), 3.69 (t,  $J = 7.6$  Hz, 2H); <sup>13</sup>C NMR (100 MHz, CDCl<sub>3</sub>) δ 164.2, 153.2, 143.6, 141.3, 133.9, 133.2, 131.6, 129.1, 127.9, 127.87, 127.2, 127.0, 126.5, 126.0, 125.8, 125.6, 125.1, 123.1, 120.7, 120.1, 67.7, 54.1, 52.2, 47.0, 34.1; HRMS  $m/z$  calcd for  $C_{32}H_{28}N_3O_4$  (M+H)<sup>+</sup> 518.2080, found 518.2080.

#### 4.5. General Procedure C for the synthesis of compound 4a-4d

##### 4.5.1. 4-[(9-Fluoren-9-ylmethoxy)carbonylamino]-1-(2-ethylbutyl)-1H-pyrazole-3-carboxylic acid (**4a**)

To a solution of **3a** (1.0 g, 2.23 mmol) in toluene-EtOAc (5:1, 40 mL) was added lithium iodide (1.50 g, 11.2 mmol). The resulting mixture was refluxed for 4 h. The reaction mixture was quenched with 10% aqueous HCl and extracted with EtOAc. The organic layer was washed with 10% aqueous Na<sub>2</sub>S<sub>2</sub>O<sub>3</sub>, brine and dried over Na<sub>2</sub>SO<sub>4</sub>, and concentrated in vacuo to afford **5a** as a white solid (950 mg, 98%). <sup>1</sup>H NMR (400 MHz, CDCl<sub>3</sub>) δ 8.22 (s, 1H), 7.91 (s, 1H), 7.70 (d, *J* = 7.4 Hz, 2H), 7.55 (d, *J* = 7.4 Hz, 2H), 7.34 (t, *J* = 7.4 Hz, 2H), 7.26 (t, *J* = 7.4 Hz, 2H), 4.39 (d, *J* = 7.2 Hz, 2H), 4.22 (t, *J* = 7.0 Hz, 1H), 3.99 (d, *J* = 7.2 Hz, 2H), 1.83 (m, 1H), 1.29-1.21 (m, 4H), 0.82 (t, *J* = 7.4 Hz, 6H); <sup>13</sup>C NMR (100 MHz, CDCl<sub>3</sub>) δ 166.7, 153.3, 143.6, 141.3, 128.6, 127.9, 127.2, 126.1, 125.1, 121.4, 120.1, 67.9, 57.0, 47.0, 41.6, 23.1, 10.5; HRMS *m/z* calcd for C<sub>25</sub>H<sub>28</sub>N<sub>3</sub>O<sub>4</sub> (M+H)<sup>+</sup> 434.2080, found 434.2080.

##### 4.5.2. 4-[(9-Fluoren-9-ylmethoxy)carbonylamino]-1-(3-phenylpropyl)-1H-pyrazol-3-carboxylic acid (**4b**).

Compound **4b** was prepared from compound **3b** following the general procedure C (white solid, 99%). <sup>1</sup>H NMR (400 MHz, CDCl<sub>3</sub>) δ 8.31 (s, 1H), 7.98 (s, 1H), 7.76 (d, *J* = 7.4 Hz, 2H), 7.61 (d, *J* = 7.4 Hz, 2H), 7.40 (t, *J* = 7.4 Hz, 2H), 7.34-7.11 (m, 7H), 4.45 (d, *J* = 7.1 Hz, 2H), 4.28 (t, *J* = 7.1 Hz, 1H), 4.15 (t, *J* = 7.2 Hz, 2H), 2.62 (t, *J* = 7.2 Hz, 2H), 2.22 (m, 2H); <sup>13</sup>C NMR (100 MHz, CDCl<sub>3</sub>) δ 166.7, 153.3, 143.6, 141.3, 140.3, 128.9, 128.6, 128.4, 127.9, 127.2,

126.3, 126.2, 125.1, 121.0, 120.1, 67.9, 53.0, 47.0, 32.6, 31.7; HRMS  $m/z$  calcd for  $C_{28}H_{26}N_3O_4$  (M+H)<sup>+</sup> 468.1923, found 468.1924.

4.5.3 4-[(9-Fluoren-9-ylmethoxy)carbonylamino]-1-(3,3-phenylpropyl)-1H-pyrazol-3-carboxylic acid (**4c**)

Compound **4c** was prepared from compound **3c** following the general procedure C (white solid, 98%). <sup>1</sup>H NMR (400 MHz, CDCl<sub>3</sub>) δ 8.29 (s, 1H), 7.91 (s, 1H), 7.76 (d,  $J = 7.4$  Hz, 2H), 7.62 (d,  $J = 7.4$  Hz, 2H), 7.40 (t,  $J = 7.4$  Hz, 2H), 7.34-7.16 (m, 12H), 4.46 (d,  $J = 7.2$  Hz, 2H), 4.28 (t,  $J = 7.2$  Hz, 1H), 4.09 (t,  $J = 7.2$  Hz, 2H), 3.88 (t,  $J = 7.8$  Hz, 1H), 2.65 (m, 2H); <sup>13</sup>C NMR (100 MHz, CDCl<sub>3</sub>) δ 166.4, 153.2, 143.6, 143.2, 141.3, 129.0, 128.8, 127.9, 127.7, 127.2, 126.7, 126.1, 125.1, 121.2, 120.1, 67.9, 52.2, 48.4, 47.0, 35.9; HRMS  $m/z$  calcd for  $C_{34}H_{30}N_3O_4$  (M+H)<sup>+</sup> 544.2236, found 544.2236.

4.5.4 4-[(9-Fluoren-9-ylmethoxy)carbonylamino]-1-[2-(naphthalen-1-yl)ethyl]-1H-pyrazole-3-carboxylic acid (**4d**)

Compound **4d** was prepared from compound **3d** following the general procedure C (white solid, 98%). <sup>1</sup>H NMR (400 MHz, CDCl<sub>3</sub>) δ 8.20 (s, 1H), 7.95 (d,  $J = 8.2$  Hz, 1H), 7.85 (s, 1H), 7.80 (d,  $J = 7.9$  Hz, 1H), 7.71-7.69 (m, 3H), 7.54 (d,  $J = 7.4$  Hz, 2H), 7.50-7.41 (m, 2H), 7.36-7.25 (m, 5H), 7.20 (d,  $J = 6.8$  Hz, 1H), 4.45 (t,  $J = 7.7$  Hz, 2H), 4.38 (d,  $J = 7.1$  Hz, 2H), 4.21 (t,  $J = 7.1$  Hz, 1H), 3.60 (t,  $J = 7.7$  Hz, 2H); <sup>13</sup>C NMR (100 MHz, CDCl<sub>3</sub>) δ 166.7, 153.2, 143.6, 141.3, 133.9, 133.1, 131.6, 129.1, 127.95, 127.9, 127.2, 127.1, 126.5, 126.2, 125.9, 125.6, 125.1, 123.0, 121.3, 120.1, 67.9, 54.2, 47.0, 34.1; HRMS  $m/z$  calcd for  $C_{31}H_{26}N_3O_4$  (M+H)<sup>+</sup> 504.1923, found 504.1923.

#### 4.6. Peptidomimetic synthesis

Rink amide 4-methylbenzhydrylamine (MBHA) resin and Fmoc-amino acids were obtained from Calbiochem-Novabiochem (La Jolla, CA). All peptides were prepared by Fmoc-based solid-phase peptide synthesis using Rink amide resin with an initial loading of 0.61 mmol/g. Resins were swollen in DMF for 45 min before synthesis. For sequence extension, the Fmoc-Arg (pbf)-OH (5.0 eq.) along with HBTU (5.0 eq.), HOBT (5.0 eq.) was added to the free amine on resin in the presence of DIEA (5.0 eq.) in DMF (2 mL) and allowed to proceed for 1 h with Vortex stirring. After washing with DMF, Fmoc deprotection was achieved with 20% piperidine in DMF (1 x 10 min, 2 x 3 min). The resin was washed once again, and the process was repeated for the next amino acid and finally the resin was washed with DMF, dichloromethane, and ether, and then dried under vacuum. The peptide cleavage from the resin and the deprotection was carried out using a mixture of trifluoroacetic acid, water, and triisopropylsilane (90:5:5, v/v/v, 2 mL) for 2 h. The crude peptide was precipitated by the addition of cold diethyl ether and filtered. Purification of crude peptide was carried out on the preparative Vydac C<sub>18</sub> column using an appropriate 10-90% water/acetonitrile gradient in the presence of 0.05% TFA (A: water buffer, B: acetonitrile buffer). Purified peptides (> 95%) were assessed by RP HPLC on an analytical Vydac C<sub>18</sub> column. Mass spectra of peptides were obtained using MALDI-TOF-MS (Shimadzu). Cyclic peptide was synthesized using Fmoc protection strategy. The linear side-chain protected peptide was synthesized on the Rink amide resin (0.61 mmol/g) coupled with the respective amino acids. Subsequently, Fmoc group in the *N*-terminal of the resin-bound protected peptide was removed using 20% piperidine/DMF. Then, the *N*-terminal amine was bromoacetylated using of BrCH<sub>2</sub>COOH (10.0 eq.) and DIC (5.0 eq.)

stirring for 3 h at rt. The peptide was cleaved from the resin and dissolved in 10 mL of water/CH<sub>3</sub>CN (1:1). Further to attain the basic solution, triethylamine was repeatedly added to adjust the pH 8-9. Under the basic condition, cysteine thiol in the linear peptide undergoes the nucleophilic displacement on *N*-bromoacetyl group to effect the spontaneous intramolecular cyclization. This cyclization process was monitored by HPLC. After 1 h at room temperature, 30% aq. AcOH the solution was added and lyophilized. The crude product was purified by RP-HPLC.

MS (MALDI-TOF): *m/z* **Py1** 367.2570 (M + H)<sup>+</sup>, **Py2** 523.8517 (M + H)<sup>+</sup>, **Py3** 401.2415 (M + H)<sup>+</sup>, **Py4** 557.3426 (M + H)<sup>+</sup>, **Py5** 477.2725 (M + H)<sup>+</sup>, **Py6** 633.8332 (M + H)<sup>+</sup>, **Py7** 437.2419 (M + H)<sup>+</sup>, **Py8** 593.4807 (M + H)<sup>+</sup>, **Py9** 936.9565 (M + H)<sup>+</sup>, **Py10** 1396.4418 (M + 2H)<sup>+</sup>, **Py11** 856.9093 (M + H)<sup>+</sup>, **Py12** 1013.1276 (M + 2H)<sup>+</sup>, **Py13** 1276.2438 (M + 2H)<sup>+</sup>, **Py14** 1079.4870 (M + H)<sup>+</sup>.

#### 4.7. Bacterial strains

Two types of Gram-positive bacteria (*Staphylococcus epidermidis* [KCTC 1917], and *Staphylococcus aureus* [KCTC 1621]) and two types of Gram-negative bacteria (*Escherichia coli* [KCTC 1682] and *Pseudomonas aeruginosa* [KCTC 1637]) were procured from the Korean Collection for Type Cultures (KCTC) at the Korea Research Institute of Bioscience and Biotechnology (KRIBB). Methicillin-resistant *Staphylococcus aureus* strains (MRSA; CCARM 3089, CCARM 3090, and CCARM 3095) and multidrug-resistant *Pseudomonas aeruginosa* strains (MDRPA; CCARM 2095, and CCARM 2109) were obtained from the Culture Collection of Antibiotic-Resistant Microbes (CCARM) at Seoul Women's University in Korea.

Vancomycin-resistant *Enterococcus faecium* (VREF; ATCC 51559) was supplied from the American Type Culture Collection (Manassas, VA, USA)

#### 4.8. Antimicrobial assay

The antimicrobial activity of the peptides against bacteria was examined using the broth microdilution method in sterile 96-well plates. Aliquots (100  $\mu$ L) of a bacterial suspension at  $2 \times 10^6$  CFU/mL in 1% peptone were added to 100  $\mu$ L of the peptide solution (serial 2-fold dilutions in 1% peptone). After incubation for 18-20 h at 37 °C, bacterial growth inhibition was determined by measuring the absorbance at 600 nm with a microplate reader (EL 800, Bio-Tek Instruments, VT, USA). The minimal inhibitory concentration (MIC) was defined as the lowest peptide concentration that causes 100% inhibition of microbial growth. In addition, the MICs of the peptides were determined in the presence of salts.  $2 \times 10^6$  CFU/ml of *E. coli* (KCTC 1682), and *S. aureus* (KCTC 1621) were treated with peptides, while different conditions were added to LB medium, and the concentrations of physiological conditions were as follows: 150 mM NaCl, 1 mM MgCl<sub>2</sub>, and 2.5mM CaCl<sub>2</sub>. After these treatments, the procedures were same as MIC assay described above.

##### 4.8.1. Hemolytic assay against sheep red blood cells (S-RBC)

The hemolytic activity of the peptides was measured as the amount of hemoglobin released by the lysis of S-RBC. Fresh S-RBC were centrifuged, washed three times with PBS (35

mM phosphate buffer, 0.15 M NaCl, pH 7.2), dispensed into 96-well plates as 100  $\mu$ L of 4% (w/v) RBC in PBS, and 100  $\mu$ L of peptide solution was added to each well. Peptide dilutions were prepared in PBS, and the range of peptide concentrations tested went from 512  $\mu$ g/mL to 1  $\mu$ g/mL. After 1 h of incubation at 37 °C under 5% CO<sub>2</sub>, cells were centrifuged at 1000 x g for 10 min and the supernatant (100  $\mu$ L) was transferred to other 96 well plates. The absorbance values of the released hemoglobin were determined at 414 nm using a microplate reader (EL 800, Bio-Tek Instruments, VT, USA). Zero hemolysis was determined in PBS ( $A_{\text{PBS}}$ ) and 100% hemolysis was determined in 0.1% (v/v) Triton X-100 ( $A_{\text{triton}}$ ). The hemolysis percentage was calculated as  $100 \times [(A_{\text{sample}} - A_{\text{PBS}}) / (A_{\text{triton}} - A_{\text{PBS}})]$ .

#### 4.8.2. Mammalian cell cultures

RAW264.7 and NIH-3T3 cells were purchased from the American Type Culture Collection (Manassas, VA), and cultured in DMEM supplemented with 10% fetal bovine serum and antibiotic-antimycotic solution (100 units/mL penicillin, 100  $\mu$ g/mL streptomycin and 25  $\mu$ g/mL amphotericin B) in 5% CO<sub>2</sub> at 37 °C. Cultures were passed every 3 to 5 days, and cells were detached by brief trypsin treatment and visualized with an inverted microscope.

#### 4.8.3. Cytotoxicity against mammalian cells

Cytotoxicity of peptides against RAW264.7 and NIH-3T3 cells was determined using the MTT proliferation assay as reported previously with minor modifications [48]. The cells were seeded on 96-well microplates at a density of  $2 \times 10^4$  cells/well in 150  $\mu$ L DMEM containing

10% fetal bovine serum. Plates were incubated for 24 h at 37 °C in 5% CO<sub>2</sub>. Peptide solutions (20 µL) (serial 2-fold dilutions in DMEM) were added, and the plates further incubated for 2 days. Wells containing cells without peptides served as controls. Subsequently, 20 µL MTT solution (5 mg/mL) was added in each well, and the plates were incubated for a further 4 h at 37 °C. Precipitated MTT formazan was dissolved in 40 µL of 20% (w/v) SDS containing 0.01 M HCl for 2h. Absorbance at 570 nm was measured using a microplate ELISA reader (Molecular Devices, Sunnyvale, CA). Cell survival was expressed as a percentage of the ratio of A<sub>570</sub> of cells treated with peptide to that of cells only.

#### 4.8.4. Protease stability by radial diffusion assay

*E. coli* (KCTC 1682) and *S. aureus* (KCTC 1621) were grown overnight for 18 h at 37 °C in 10 mL of LB broth, and then 10 mL of this culture was inoculated into 10 mL of fresh LB and incubated for an additional 3 h at 37 °C to obtain mid-logarithmic-phase organisms. A bacteria suspension ( $2 \times 10^6$  CFU/ml in LB) was mixed with 0.7% agarose. This mixture was poured into a 10-cm petri dish, and it dispersed rapidly. Five microliters of an aqueous peptide stock solution (10 mg/mL) were added to 25 mL of trypsin solution in PBS (0.2 µg/mL), and incubated at 37 °C for 4 h. The reaction was stopped by freezing with liquid nitrogen, after which 10 µL aliquots were placed in each circle paper (< 6 mm in diameter), put on the agarose plates, and then incubated at 37 °C overnight. The diameters of the bacterial clearance zones surrounding the circle paper were measured for the quantitation of inhibitory activities.

#### 4.8.5. Inhibition of biofilm formation

MDRPA 2095 strain ( $1 \times 10^6$  cfu/mL) in MHB containing 0.2% glucose were incubated at 37 °C, 24 h with or without peptides (serial two-fold dilutions ranging from 1 µg/mL to 64 µg/mL) in 96-well tissue culture microtiter plates. Six wells were used for each peptide or control. After the incubation, the waste media was aspirated gently. The wells of the plates were washed three times with 250 µL physiological buffered saline (PBS) solutions to remove unattached bacteria and air-dried. 200 µL of 99% methanol was added per well for 15 min for fixation and aspirated, and plates were allowed to dry. Wells were stained with 100 µL of 0.1% crystal violet for 5 min. Excess stain was gently rinsed off with tap water, and plates were air-dried. The stain was resolubilized in 100 µL of 95% ethanol, shaking in orbital shaker for 30 min and measured the absorbance at 600 nm.

#### 4.8.6. Membrane depolarization

The cytoplasmic membrane depolarization activity of the peptides was measured using the membrane potential sensitive dye, diSC<sub>3-5</sub> as previously described [49,50]. Briefly, *S. aureus* (KCTC 1621) grown at 37 °C, with agitation, to the mid-log phase ( $OD_{600} = 0.4$ ) was harvested by centrifugation. Cells were washed twice with washing buffer (20 mM glucose, 5 mM HEPES, pH 7.4) and resuspended to an  $OD_{600}$  of 0.05 in similar buffer. The cell suspension was incubated with 20 nM diSC<sub>3-5</sub> until a stable fluorescence value was achieved, which implied the full incorporation of the dye into the bacterial membrane. Membrane depolarization was monitored through the changes in the intensity of fluorescence emission of the membrane potential-sensitive

dye, diSC<sub>3-5</sub> (excitation  $\lambda = 622$  nm, emission  $\lambda = 670$  nm) after peptide addition. The membrane potential was fully abolished by adding gramicidin D (final concentration of 0.2 nM).

#### 4.8.7. Outer membrane permeability assay

The ability of peptides to increase outer membrane permeability of Gram-negative bacteria was determined by measuring incorporation of the fluorescent dye NPN into the outer membrane of *E. coli* (KCTC 1682) as previously described [51–53]. Briefly, *E. coli* cells were suspended to a final concentration of OD<sub>600</sub> = 0.05 in 5 mM HEPES buffer, pH 7.2, containing 5 mM KCN. NPN was added to 3 mL of cells in a quartz cuvette to give a final concentration of 10  $\mu$ M and the background fluorescence recorded (excitation  $\lambda = 350$  nm, emission  $\lambda = 420$  nm) with RF-5301PC spectrofluorophotometer (Shimadzu, Japan). Aliquots of peptide were added to the cuvette, and the fluorescence was recorded as a function of time until there was no further increase in fluorescence. As outer membrane permeability is increased by the addition of peptide, NPN incorporated into the membrane causes an increase in fluorescence.

#### 4.8.8. Inner membrane permeability assay

The inner membrane permeability of peptides was determined by measurement in *E. coli* ML-35 of  $\beta$ -galactosidase activity using the normally impermeable, chromogenic substrate ONPG as a substrate, which has been described previously [54,55]. *E. coli* ML-35 were washed in 10 mM sodium phosphate (pH 7.4) containing 100 mM NaCl and resuspended in the same

buffer at a final concentration of  $OD_{600} = 0.5$  containing 1.5 mM ONPG. The hydrolysis of ONPG to o-nitrophenol over the time was monitored spectrophotometrically at 405 nm following the addition of peptide samples.

#### 4.8.9. Transmission electron microscope (TEM)

Morphological changes of *E. coli* (KCTC 1682) and *S. aureus* (KCTC 1621) after the addition of Py11 were analyzed using TEM. The bacterial culture at  $2 \times 10^7$  CFU/mL in LB media was washed three times in PBS via a series of centrifugation at  $10,000 \times g$ , for 5 min, and re-suspension. One-hundred microliters of Py11 in PBS were added to an equal volume of bacterial suspension to a final concentration at  $2 \times$  MIC. Following the addition of Py11, the samples were incubated for 1 h at 37 °C. Bacterial cell pellet after centrifugation was re-suspended in 20 mL PBS for TEM specimen preparation. Five microliters of sample solution were loaded onto a carbon film-coated TEM grid, which was rendered hydrophilic by glow discharge. After 90 s, the excess sample solution was washed off with distilled water. Five microliters of 1% uranyl acetate were loaded onto the grid for negative staining for 1 min, and excess stain solution was blotted using a piece of filter paper. Samples were imaged using a Tecnai G<sup>2</sup> Spirit electron microscope (FEI) equipped with a lanthanum hexaboride (Lab6) gun, operating at 120 kV. Images were recorded using the Ultrascan 4000 charge-coupled device (CCD) camera (Gatan).

#### 4.8.10 Nitric oxide (NO) release from LPS-stimulated RAW264.7 cells

RAW264.7 macrophage cells were plated at a density of  $5 \times 10^5$  cells/mL in 96-well culture plates and stimulated with LPS (20 ng/mL) in the presence or absence of peptides for 24 h. Isolated supernatant fractions were mixed with an equal volume of Griess reagent (1% sulfanilamide, 0.1% naphthylethylenediamine dihydrochloride, and 2% phosphoric acid) and incubated at room temperature for 10 min. Nitrite production was measured by absorbance at 540 nm, and concentrations were determined using a standard curve generated with  $\text{NaNO}_2$ .

#### 4.8.11. *TNF- $\alpha$ release from LPS-stimulated RAW264.7 cells*

RAW264.7 cells were seeded in 96-well plates ( $5 \times 10^4$  cells/well) and incubated overnight. Peptides were added and incubated at 37 °C. After washing for five times with PBS to remove unbound peptides, LPS (20 ng/mL) was added and incubated for 6 h at 37 °C. The concentration of TNF- $\alpha$  or IL-6 in the samples was measured using a mouse TNF- $\alpha$  enzyme-linked immunosorbent assay (ELISA) kit (R&D Systems, Minneapolis, MN, USA) according to the manufacturer's protocol.

#### 4.8.12. *Reverse transcription-polymerase chain reaction (RT-PCR)*

RAW264.7 cells were plated at  $5 \times 10^5$  cells/well in six-well plates and cultured overnight. Cells were stimulated for 3 h (for TNF- $\alpha$ ) or 6 h (for iNOS) without (negative control) or with 20 ng/mL LPS in the presence or absence of peptide in DMEM supplemented with 10% bovine serum. The cells were detached from the wells and washed once with phosphate-buffered saline.

Total RNA was prepared, and reverse transcribed to cDNA with oligo (dT) 15 primers. The cDNA products were amplified in the presence of primers for iNOS (forward, 5'-CTGCAGCACTTGGATCAGGAACCTG-3'; reverse, 5'-GGGAGTAGCCTGTGTGCACCTGGAA-3'); TNF- $\alpha$  (forward, 5'-CCTGTAGCCCACGTCGTAGC-3'; reverse, 5'-TTGACCTCAGCGCTGAGTTG-3'); and  $\beta$ -actin (forward, 5'-TGGAATCCTGTGGCATCCATGAAAC-3'; reverse, 5'-TAAAACGCAGCTCAGTAACAGTCCG-3'). The amplification protocol consisted of an initial denaturation at 94 °C for 5 min, followed by 30 cycles of denaturation at 94 °C for 1 min, annealing at 55 °C for 1.5 min, and extension at 72 °C for 1 min, with a final extension at 72 °C for 5 min.

### Statistical analysis

Data were analyzed by ANOVA using SigmaPlot 12.0 software. Quantitative data are presented as the mean  $\pm$  standard deviation of the mean. Differences were defined as significant at a P-value of less than 0.001.

### Acknowledgments

This work was supported by the Korea Basic Science Institute's Research Program grant T36412 (J.K.B.), R&D Convergence Program of National Research Council of Science & Technology (J.K.B.), National Research Foundation of Korea (NRF) grant (S.J.L.) funded by the

Korea government (MEST) (2011-0017405), Basic Science Research Program through the National Research Foundation of Korea (NRF) funded the Ministry of Education (2015R1D1A1A01057988) (S.Y.S), National Research Foundation of Korea (NRF) grants funded by the Ministry of Science, ICT & Future Planning (MSIP) of Korea (NRF-2014R1A4A1007304 to Y.H.J.) and the Next-Generation BioGreen 21 Program (#PJ009594), Rural Development Administration (N.H.K.).

**References**

- [1] M.S. Butler, M.A. Blaskovich, M.A. Cooper, Antibiotics in the clinical pipeline in 2013, *J. Antibiot.* 66 (2013) 571–591.
- [2] M. Zasloff, Antimicrobial peptides of multicellular organisms, *Nature* 415 (2002) 389–395.
- [3] U. Theuretzbacher, Accelerating resistance, inadequate antibacterial drug pipelines and international responses, *Int. J. Antimicrob. Agents* 39 (2012) 295–299.
- [4] S.B. Levy, B. Marshall, Antibacterial resistance worldwide: causes, challenges and responses. *Nat. Med.* 10 (2004) S122–129.
- [5] B. Spellberg, J. H. Powers, E.P. Brass, L.G. Miller, J.E. Jr. Edwards, Trends in antimicrobial drug development: implications for the future. *Clin. Infect. Dis.* 38 (2004) 1279–1286.
- [6] J.K. Kim, E. Lee, S. Shin, K.W. Jeong, J.Y. Lee, S.Y. Bae, S.H. Kim, J. Lee, S. Kim, D. Lee, J.S. Hwang, Y. Kim, Structure and function of papiliocin with antimicrobial and anti-inflammatory activities isolated from the swallowtail butterfly, *papilio xuthus*, *J. Biol. Chem.* 286 (2011) 41296–41311.
- [7] R. Bals, J.M. Wilson, Cathelicidins—a family of multifunctional antimicrobial peptides, *Cell. Mol. Life Sci.* 60 (2003) 711–720.
- [8] T. Ganz, Defensins: antimicrobial peptides of innate immunity, *Nat. Rev. Immunol.* 3 (2003) 710–720.
- [9] Y. Lai, R.L. Gallo, AMPed up immunity: how antimicrobial peptides have multiple roles in immune defense, *Trends Immunol.* 30 (2009) 131–141.

- [10] R.E. Hancock, M.G. Scott, The role of antimicrobial peptides in animal defenses, *Proc. Natl. Acad. Sci. U.S.A.* 97 (2000) 8856–8861.
- [11] P. Dutta, S. Das, Mammalian antimicrobial peptides: promising therapeutic targets against infection and chronic inflammation. *Curr. Top. Med. Chem.* 16 (2016) 99–129.
- [12] Y. Lai, R.L. Gallo, AMPed up immunity: how antimicrobial peptides have multiple roles in immune defense. *Trends Immunol.* 30 (2009) 131–141.
- [13] R.E. Hancock, H.G. Sahl, New strategies and compounds for anti-infective treatment. *Curr. Opin. Microbiol.* 16 (2013) 519–521.
- [14] N.F. Von, M. Brands, B. Hinzen, S. Weigand, D. Habich, Antibacterial natural products in medicinal chemistry-exodus or revival?, *Angew. Chem. Int. Ed.* 45 (2006) 5072–5129.
- [15] R. Hancock, M.G. Scott, The role of antimicrobial peptides in animal defenses, *Proc. Natl. Acad. Sci. U. S. A.* 97 (2000) 8856–8861.
- [16] A.T.Y. Yeung, S.L. Gellatly, R.E.W. Hancock, Multifunctional cationic host defense peptides and their clinical applications, *Cell. Mol. Life Sci.* 68 (2011) 2161–2176.
- [17] B.M. Peters, M.E. Shirtliff, M.A. Jabra-Rizk, Antimicrobial peptides: primeval molecules or future drugs? *PLoS Pathog.* 6 (2010) e1001067.
- [18] G. Bell, P.H. Gouyon, Arming the enemy: the evolution of resistance to self-proteins, *Microbiology* 149 (2003) 1367–1375.
- [19] N.P. Chongsiriwatana, J.A. Patch, A.M. Czyzewski, M.T. Dohm, A. Ivankin, D. Gidalevitz, R.N. Zuckermann, A.E. Barron, Peptoids that mimic the structure, function, and mechanism of helical antimicrobial peptides, *Proc. Natl. Acad. Sci. U. S. A.* 105 (2008) 2794–2799.

- [20] C.A. Olsen, H.L. Ziegler, H.M. Nielsen, N. Frimodt-Møller, J.W. Jaroszewski, H. Franzyk, Antimicrobial, hemolytic, and cytotoxic activities of beta-peptoid-peptide hybrid oligomers: improved properties compared to natural AMPs, *ChemBioChem*. 11 (2010) 1356–1360.
- [21] R. Kapoor, M.W. Wadman, M.T. Dohm, A.M. Czyzewski, A.M. Spormann, A.E. Barron, Antimicrobial peptoids are effective against *Pseudomonas aeruginosa* biofilms, *Antimicrob. Agents Chemother.* 55 (2011) 3054–3057.
- [22] M.L. Huang, S.B. Shin, M.A. Benson, V.J. Torres, K. Kirshenbaum, A comparison of linear and cyclic peptoid oligomers as potent antimicrobial agents, *ChemMedChem*. 7 (2012) 114–122.
- [23] A.J. Karlsson, R.M. Flessner, S.H. Gellman, D.M. Lynn, S.P. Palecek, Polyelectrolyte multilayers fabricated from antifungal  $\beta$ -peptides: design of surfaces that exhibit antifungal activity against *Candida albicans*, *Biomacromolecules* 11 (2010) 2321–2328.
- [24] J. Hua, R.W. Scott, G. Diamond, Activity of antimicrobial peptide mimetics in the oral cavity: II. Activity against periopathogenic biofilms and anti-inflammatory activity, *Mol. Oral. Microbiol.* 25 (2010) 426–432.
- [25] P. Claudon, A. Violette, K. Lamour, M. Decossas, S. Fournel, B. Heurtault, J. Godet, H. Mély, B. Jamart-Grégoire, M.C. Averlant-Petit, J.P. Briand, G. Duportail, H. Monteil, G. Guichard, Consequences of isostructural main-chain modifications for the design of antimicrobial foldamers: helical mimics of host-defense peptides based on a heterogeneous amide/urea backbone, *Angew. Chem. Int. Ed.* 49 (2010) 333–336.
- [26] N. Srinivas, P. Jetter, B.J. Ueberbacher, M. Werneburg, K. Zerbe, J. Steinmann, B. Van der Meijden, F. Bernardini, A. Lederer, R.L. Dias, P.E. Misson, H. Henze, J. Zumbrunn, F.O. Gombert, D. Obrecht, P. Hunziker, S. Schauer, U. Ziegler, A. Käch, L. Eberl, K. Riedel, S.

- J. DeMarco, J.A. Robinson, Peptidomimetic antibiotics target outer-membrane biogenesis in *Pseudomonas aeruginosa*, *Science* 327 (2010) 1010–1013.
- [27] A. Makovitzki, J. Baram, Y. Shai, Ultrashort antibacterial and antifungal lipopeptides, *Proc. Natl. Acad. Sci. U. S. A.* 103 (2006) 15997–16002.
- [28] M. Ahn, B. Jacob, P. Gunasekaran, R.N. Murugan, E.K. Ryu, G. Lee, J.K. Hyun, C. Cheong, N.H. Kim, S.Y. Shin, J. K. Bang, Poly-lysine peptidomimetics having potent antimicrobial activity without hemolytic activity, *Amino acids* 46 (2014) 2259–2269.
- [29] R.N. Murugan, B. Jacob, M. Ahn, E. Hwang, H. Sohn, H.N. Park, E. Lee, J.H. Seo, C. Cheong, K.Y. Nam, J.K. Hyun, K.W. Jeong, Y. Kim, S.Y. Shin, J.K. Bang, De Novo Design and Synthesis of Ultra-Short Peptidomimetic Antibiotics Having Dual Antimicrobial and Anti-Inflammatory Activities, *PLoS One* 8 (2013) e80025.
- [30] R.N. Murugan, B. Jacob, E.H. Kim, M. Ahn, J.H. Seo, C. Cheong, J.K. Hyun, K.S. Lee, S.Y. Shin, J.K. Bang, Non hemolytic short peptidomimetics as a new class of potent and broad-spectrum antimicrobial agents, *Bioorg. Med. Chem. Lett.* 23 (2013) 4633–4636.
- [31] M. Ahn, R.N. Murugan, B. Jacob, J.K. Hyun, C. Cheong, E. Hwang, H.N. Park, J.H. Seo, G. Srinivasrao, K.S. Lee, S.Y. Shin, J.K. Bang, Discovery of novel histidine-derived lipopeptides: applied in the synthesis of ultra-short antimicrobial peptidomimetics having potent antimicrobial activity, salt resistance and protease stability, *Eur. J. Med. Chem.* 68 (2013) 10–18.
- [32] V. Hernandez-Gordillo, I. Geisler, J. Chmielewski, Dimeric unnatural polyproline-rich peptides with enhanced antibacterial activity, *Bioorg. Med. Chem. Lett.* 24 (2014) 556–559.

- [33] M.F. Khan, M.M. Alam, G. Verma, W. Akhtar, M. Akhter, M. Shaquiquzzman, The therapeutic voyage of pyrazole and its analogs: A review, *Eur. J. Med. Chem.* 120 (2016) 170–201.
- [34] E. Lee, J.K. Kim, D. Jeon, K.W. Jeong, A. Shin, Y. Kim, Functional Roles of Aromatic Residues and Helices of Papiliocin in its Antimicrobial and Anti-inflammatory Activities, *Sci. Rep.* 5 (2015) 12048.
- [35] E.M. Driggers, S.P. Hale, J. Lee, N.K. Terrett, The exploration of macrocycles for drug discovery - an underexploited structural class, *Nat. Rev. Drug Discovery* 7 (2008) 608–624.
- [36] J. Svenson, W. Stensen, B.O. Brandsdal, B.E. Haug, J. Monrad, J.S. Svendsen, Antimicrobial peptides with stability toward tryptic degradation, *Biochemistry* 47 (2008) 3777–3788.
- [37] T. Bjarnsholt, O. Ciofu, S. Molin, M. Givskov, N. Høiby, Applying insights from biofilm biology to drug development—can a new approach be developed? *Nat. Rev. Drug Discov.* 12 (2013) 791–808.
- [38] E. Hell, C.G. Giske, A. Nelson, U. Romling, G. Marchini, Human cathelicidin peptide LL 37 inhibits both attachment capability and biofilm formation of *Staphylococcus epidermidis*. *Lett. Appl. Microbiol.* 50 (2010) 211–215.
- [39] J. Overhage, A. Campisano, M. Bains, E.C. Torfs, B.H. Rehm, R.E. Hancock, Human hostdefense peptide LL-37 prevents bacterial biofilm formation. *Infect. Immun.* 76 (2008) 4176–4182.
- [40] ET. Rietschel, H. Brade, O. Holst, L. Brade, S. Muller-Loennies, U. Mamat, U. Zahringer, F. Beckmann, U. Seydel, K.Brandenburg, A.J. Ulmer, T. Mattern, H. Heine, J. Schletter, H.

- Loppnow, U. Schonbeck, H.D. Flad, S. Hauschildt, U.F. Schade, F. Di Padova, S. Kusumoto, R.R. Schumann, Bacterial endotoxin: chemical constitution, biological recognition, host response, and immunological detoxification. *Curr. Top Microbiol. Immunol.* 216 (1996) 39–81.
- [41] C.A. Dinarello, Proinflammatory and anti-inflammatory cytokines as mediators in the pathogenesis of septic shock. *Chest* 112 (1997) 321S–329S.
- [42] M. Gough, R.E. Hancock, N.M. Kelly, Antiendotoxin activity of cationic peptide antimicrobial agents, *Infect. Immun.* 64 (1996) 4922–4927.
- [43] Y. Rosenfeld, Y. Shai, Lipopolysaccharide (endotoxin)-host defense antibacterial peptides interactions: role in bacterial resistance and prevention of sepsis. *Biochim. Biophys. Acta* 1758 (2006) 1513–1522.
- [44] Y. Rosenfeld, N. Papo, Y. Shai, Endotoxin (lipopolysaccharide) neutralization by innate immunity host-defense peptides. Peptide properties and plausible modes of action. *J. Biol. Chem.* 281 (2006) 1636–1643.
- [45] S. Bhattacharjya, *De novo* designed lipopolysaccharide binding peptides: structure based development of antiendotoxic and antimicrobial drugs. *Curr. Med. Chem.* 17 (2010) 3080–3093.
- [46] E.K. Lee, Y.C. Kim, Y.H. Nan, S.Y. Shin, Cell selectivity, mechanism of action and LPS-neutralizing activity of bovine myeloid antimicrobial peptide-18 (BMAP-18) and its analogs. *Peptides* 32 (2011) 1123–1130.
- [47] D. Pulido, M.V. Nogues, E. Boix, M. Torrent, Lipopolysaccharide neutralization by antimicrobial peptides: a gambit in the innate host defense strategy. *J. Innate Immun.* 4

- (2012) 327–336.
- [48] D.A. Scudiero, R.H. Shoemaker, K.D. Paull, A. Monks, S. Tierney, T.H. Nofziger, M.J. Currens, D. Seniff, M.R. Boyd, Evaluation of a soluble tetrazolium/formazan assay for cell growth and drug sensitivity in culture using human and other tumor cell lines, *Cancer Res.* 48 (1998) 4827–4833.
- [49] M. Wu, E. Maier, R. Benz, R.E. Hancock, Mechanism of interaction of different classes of cationic antimicrobial peptides with planar bilayers and with the cytoplasmic membrane of *Escherichia coli*, *Biochemistry* 38 (1998) 7235–7242.
- [50] C.L. Friedrich, D. Moyles, T.J. Beveridge, R.E. Hancock, Antibacterial action of structurally diverse cationic peptides on gram-positive bacteria, *Antimicrob. Agents Chemother.* 44 (2000) 2086–2092.
- [51] B. Loh, C. Grant, R.E. Hancock, Use of the fluorescent probe 1-N-phenyl-naphthylamine to study the interactions of aminoglycoside antibiotics with the outer membrane of *Pseudomonas aeruginosa*, *Antimicrob. Agents Chemother.* 26 (1984) 546–551.
- [52] R.E. Hancock, S.W. Farmer, Mechanism of uptake of deglucoteicoplanin amide derivatives across outer membranes of *Escherichia coli* and *Pseudomonas aeruginosa*, *Antimicrob. Agents Chemother.* 37 (1993) 453–456.
- [53] S. Ono, S. Lee, Y. Kadera, H. Aoyagi, M. Waki, T. Kato, N. Izumiya, Environment-dependent conformation and antimicrobial activity of a gramicidin S analog containing leucine and lysine residues, *FEBS Lett.* 220 (1987) 332–336.
- [54] R.I. Lehrer, A. Barton, K.A. Daher, S.S. Harwig, T. Ganz, M.E. Selsted, Interaction of human defensins with *Escherichia coli* mechanism of bactericidal activity. *J. Clin. Invest.* 84 (1989) 553–561.

- [55] B. Skerlavaj, D. Romeo, R. Gennaro, Rapid membrane permeabilization and inhibition of vital functions of gram-negative bacteria by bactenecins, *Infect. Immun.* 58 (1990) 3724–3730.

## Figure legends

**Scheme 1.** General synthesis of pyrazole-amino acids

Reagents and conditions: (a) thionyl chloride, MeOH, reflux, 5 h, 99%; (b) RX, K<sub>2</sub>CO<sub>3</sub>, DMF, 60 °C, 15 h, 49-67%; (c) H<sub>2</sub>, Pd/C, MeOH-CH<sub>2</sub>Cl<sub>2</sub>, 3 h; (d) Fmoc-OSu, NaHCO<sub>3</sub>, THF-H<sub>2</sub>O, rt, 3 h, 67-72% (over 2 steps); (e) LiI, toluene-EtOAc, reflux, 4 h, 98%.

**Figure 1.** Structures of the synthetic peptidomimetics

**Figure 2.** Concentration–response curves of percent hemolysis of Py11, melittin and LL-37 against sheep red blood cells (s-RBCs).

**Figure 3.** Cytotoxicity of Py11 against mouse macrophage RAW264.7 cells (A) and mouse fibroblast NIH-3T3 cells (B).

**Figure 4.** Inhibition of antimicrobial activity by trypsin, assessed by a radial diffusion assay using *E. coli* and *S. aureus*.

**Figure 5.** Inhibitory effect of Py11 and LL-37 on biofilm formation of MDRPA. Various concentrations of Py11 and LL-37 incubated with MDRPA (CCARM 2095) for 24 h. After the incubation crystal violet was used to stain the biofilm, dissolved in 95% Ethanol and absorbance (OD<sub>600</sub>) was measured. Asterisks indicate significant effects of Py11 compared to control (without peptide). Solid lines and dotted lines represent, respectively, 50 and 90 % reduction of biofilm biomass, as compared to the control biofilms. Data were analyzed by one-way ANOVA with Bonferroni's post-test ( $*P < 0.001$  for each agonist). The data are mean  $\pm$  SEM of technical triplicates, and the findings were similar when the experiments were repeated using different cells.

**Figure 6. (A)** The outer membrane permeability of *Escherichia coli* by the peptides. *E. coli* (KCTC 1682) cells were incubated with NPN in the presence of various concentrations of the peptides. Enhanced uptake of NPN was measured by an increase in fluorescence caused by partitioning of NPN into the hydrophobic interior of the outer membrane. **(B)** The inner membrane permeabilization of *E. coli* ML-35 by the peptides. Permeabilization was determined by following spectrophotometrically at 415 nm, the unmasking of cytoplasmic  $\beta$ -galactosidase activity as assessed by hydrolysis of the normally impermeable, chromogenic substrate ONPG. *E. coli* (approximately  $10^6$  colony forming units/ml) was resuspended in 10 mM sodium phosphate buffer, pH 7.5, containing 100 mM NaCl and 1.5 mM substrate.

**Figure 7.** The cytoplasmic membrane depolarization against *S. aureus* by the peptides. The cytoplasmic membrane potential variation was measured using the membrane potential-sensitive

dye diSC<sub>3</sub>-5. Dye release was monitored at an excitation wavelength of 622 nm and an emission wavelength of 670 nm as a function of time.

**Figure 8.** TEM micrographs of *E. coli*: (A) control, no peptides; (B) Py11-treated ( $2 \times \text{MIC}$ ). TEM micrographs of *S. aureus*: (C) control, no peptides; (D) Py11-treated ( $2 \times \text{MIC}$ ).

**Figure 9.** (A) Effects of Py11 on LPS-stimulated nitric oxide (NO) production in RAW264.7 cells. (B) Effects of Py11 on LPS-stimulated TNF- $\alpha$  release from RAW264.7 cells. Asterisks indicate significant effects of peptides compared to LPS treated cells. Data were analyzed by one-way ANOVA with Bonferroni's post-test ( $*P < 0.001$  for each agonist). The data are mean  $\pm$  SEM of technical triplicates, and the findings were similar when the experiments were repeated using different cells. Control represents cell only.

**Figure 10.** Effects of Py11 on the mRNA expression of iNOS and TNF- $\alpha$  in LPS-stimulated RAW264.7 cells. RAW264.7 cells ( $5 \times 10^5$  cells/well) were incubated with the peptides in the presence of LPS (20 ng/ml) for 3 h (for TNF- $\alpha$ ) or 6 h (for iNOS). Total RNA was isolated and analyzed for the expression of iNOS mRNA and TNF- $\alpha$  mRNAs by PCR. Control represents cell only.

**Table 1.** MIC values for the synthetic antimicrobial peptidomimetics used in this study

| Peptides | MIC <sup>a</sup> (µg/mL)               |  |  |   |
|----------|--|--|--|---|
|          | Gram-negative bacteria                 |  | Gram-positive bacteria                           |   |
|          | <i>Escherichia coli</i><br>(KCTC 1682) | <i>Pseudomonas aeruginosa</i><br>(KCTC 1637) | <i>Staphylococcus epidermidis</i><br>(KCTC 1917) | <i>Staphylococcus aureus</i><br>(KCTC 1621) |
| Py1      | > 64                                   | > 64   | > 64   | > 64  |
| Py2      | > 64                                   | > 64   | > 64   | > 64  |
| Py3      | > 64                                   | > 64   | > 64   | > 64  |
| Py4      | > 64                                   | > 64   | > 64   | 64  |
| Py5      | > 64                                   | 32   | > 64   | > 64  |
| Py6      | > 64                                   | 8  | > 64   | 8   |
| Py7      | > 64                                   | > 64   | > 64   | > 64  |
| Py8      | > 64                                   | > 64   | > 64   | 32  |
| Py9      | 32                                     | 32   | 32   | 8   |
| Py10     | 64                                     | > 64   | 64   | 32  |
| Py11     | 32                                     | 8  | 32   | 4   |
| Py12     | 32                                     | 8  | 32   | 4   |
| Py13     | >64                                    | > 64   | 64   | 8   |
| Py14     | >64                                    | > 64   | 64   | 16  |
| LL37     | 32                                     | 64   | 32   | 32  |
| melittin | 16                                     | 32   | 32   | 16  |

<sup>a</sup> MICs (minimal inhibitory concentrations) were determined as the lowest concentration of peptide that causes 100 % inhibition of microbial growth.

**Table 2.** Therapeutic index (TI) of Py11, LL-37 and melittin

| Peptides | GM ( $\mu\text{g/mL}$ ) <sup>a</sup> | MHC ( $\mu\text{g/mL}$ ) <sup>b</sup> | TI (MHC/GM) |
|----------|--------------------------------------|---------------------------------------|-------------|
| Py11     | 19                                   | 512 <                                 | 53.9        |
| LL-37    | 40                                   | 512 <                                 | 25.6        |
| melittin | 24                                   | 11.0                                  | 0.5         |

<sup>a</sup> GM denotes the geometric mean of MIC values from selected four bacterial strains.

<sup>b</sup> MHC is the lowest peptide concentration that produces 10% hemolysis of sheep red blood cells.

<sup>c</sup> Therapeutic index (TI) is the ratio of the MHC value ( $\mu\text{g/mL}$ ) over the GM ( $\mu\text{g/mL}$ ).

When 10% hemolysis was not observed at 512  $\mu\text{g/mL}$ , a value of 1024 $\mu\text{g/mL}$  was used for calculation of the MHC value.

**Table 3.** MIC values for Py11 and melittin against antibiotic-resistant bacteria

| Microorganisms     | MIC ( $\mu\text{g/mL}$ ) |          |
|--------------------|--------------------------|----------|
|                    | Py11                     | melittin |
| MRSA <sup>a</sup>  |                          |          |
| CCARM 3089         | 8                        | 16       |
| CCARM 3090         | 8                        | 16       |
| CCARM 3095         | 4                        | 16       |
| MDRPA <sup>b</sup> |                          |          |
| CCARM 2109         | 8                        | 32       |
| CCARM 2095         | 8                        | 32       |
| VREF <sup>c</sup>  |                          |          |
| ATCC 51559         | 8                        | 16       |

<sup>a</sup>MRSA: methicillin-resistant *Staphylococcus aureus*

<sup>b</sup>MDRPA: multidrug-resistant *Pseudomonas aeruginosa*

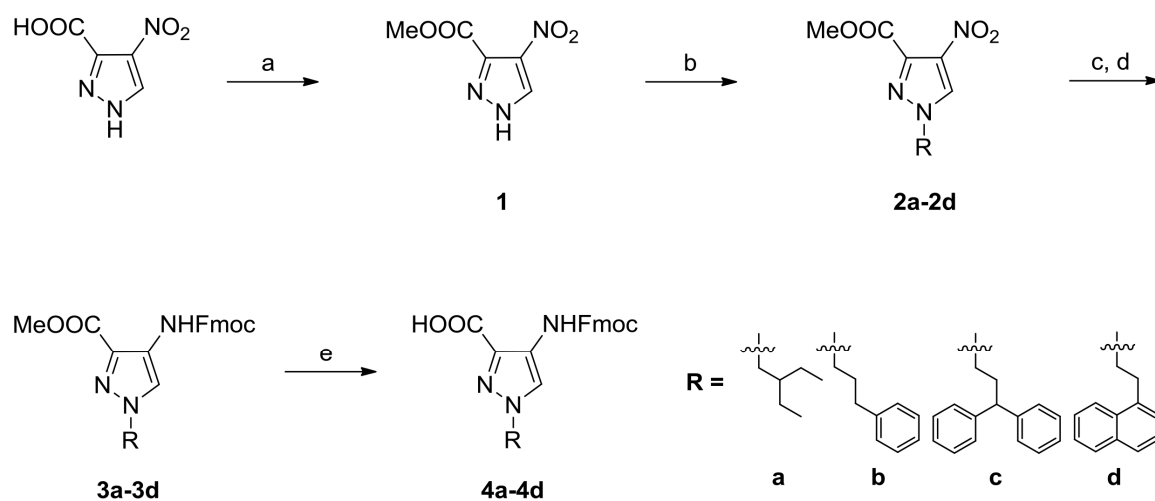
<sup>c</sup>VREF: vancomycin-resistant *Enterococcus faecium*

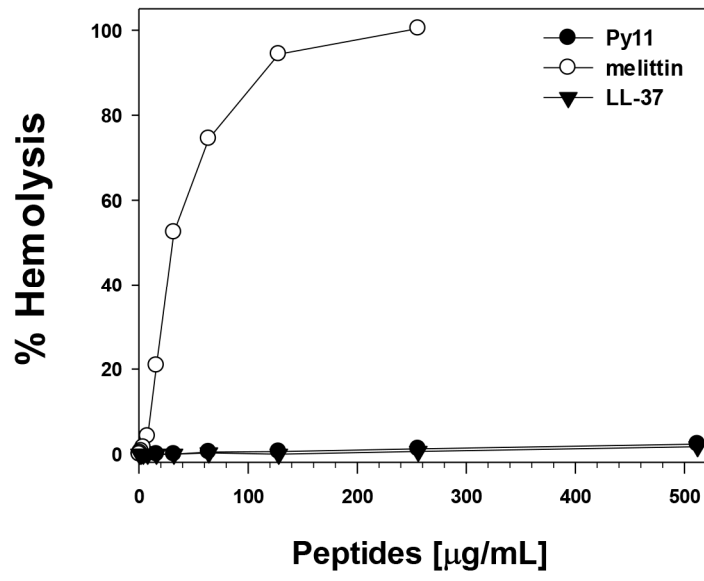
**Table 4.** MIC values of Py11 in the presence of salts against *E. coli* and *S. aureus*.

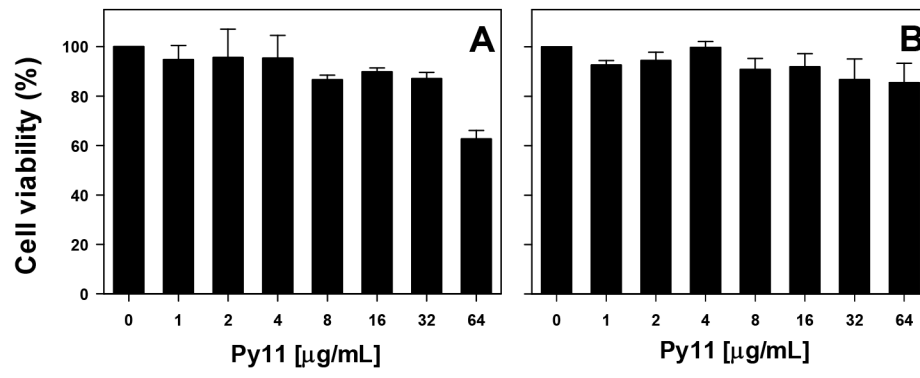
| Control   | 150 mM NaCl | 1mM MgCl <sub>2</sub> | 2.5mM CaCl <sub>2</sub> |
|---|-------------|-----------------------|-------------------------|
| MIC (µg/ml) against <i>E. coli</i> (KCTC 1682)  |             |                       |                         |
| 32  | 32          | 32                    | 32                      |
| MIC (µg/ml) against <i>S. aureus</i> (KCTC1621) |             |                       |                         |
| 4   | 4           | 8                     | 8                       |

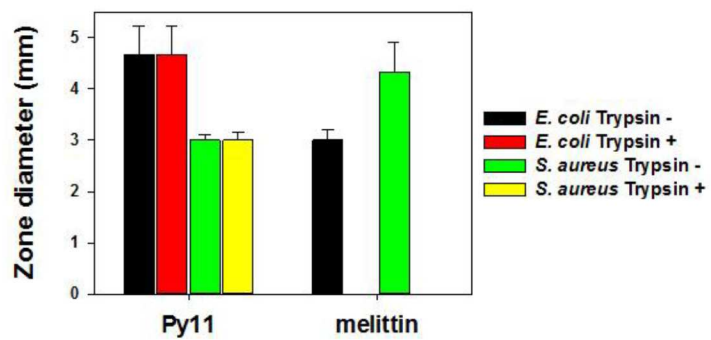
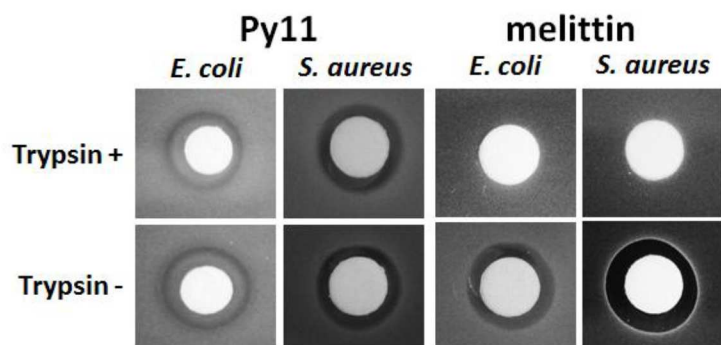
Control represents treated with peptide only.

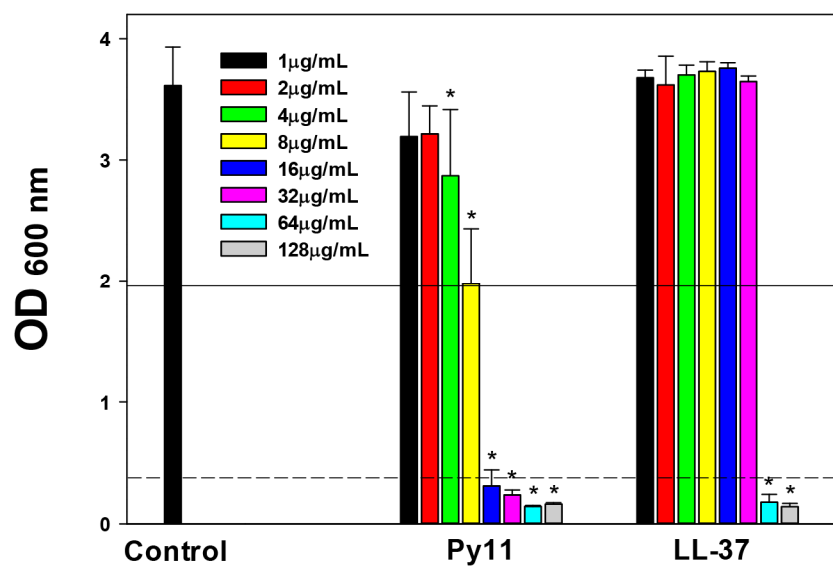


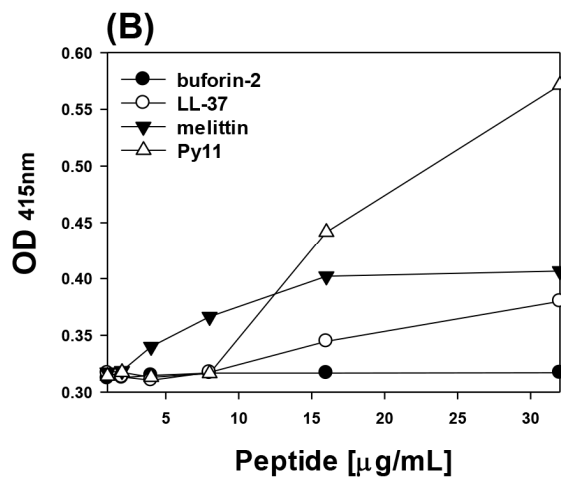
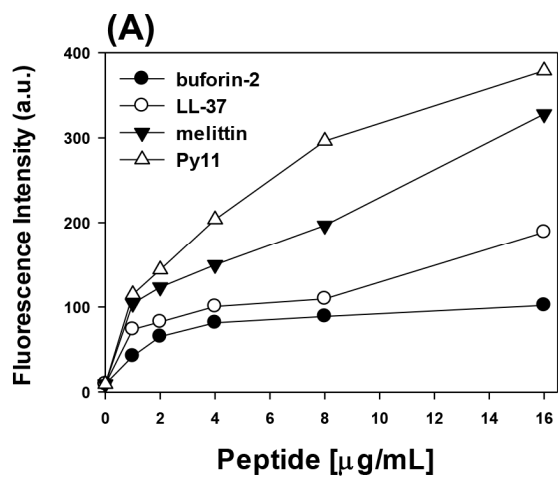


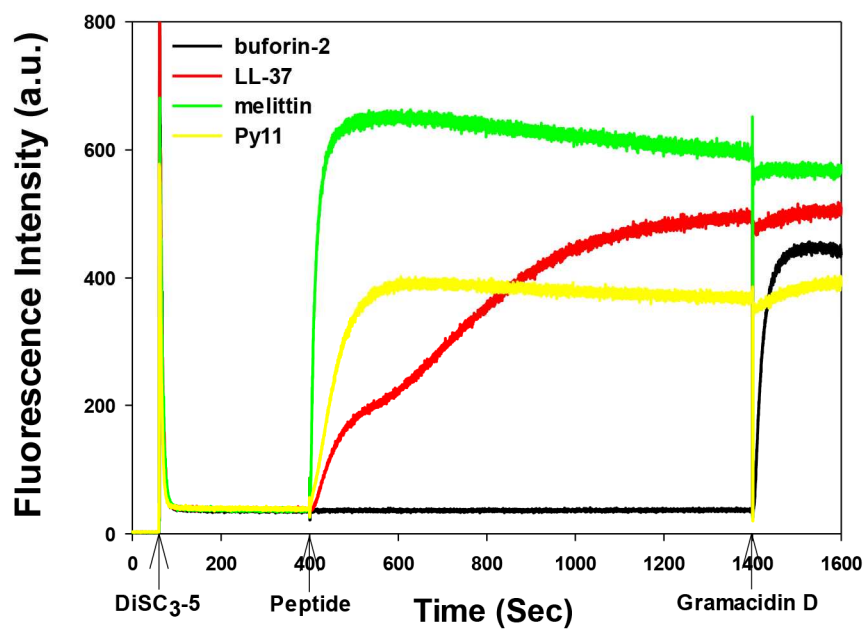


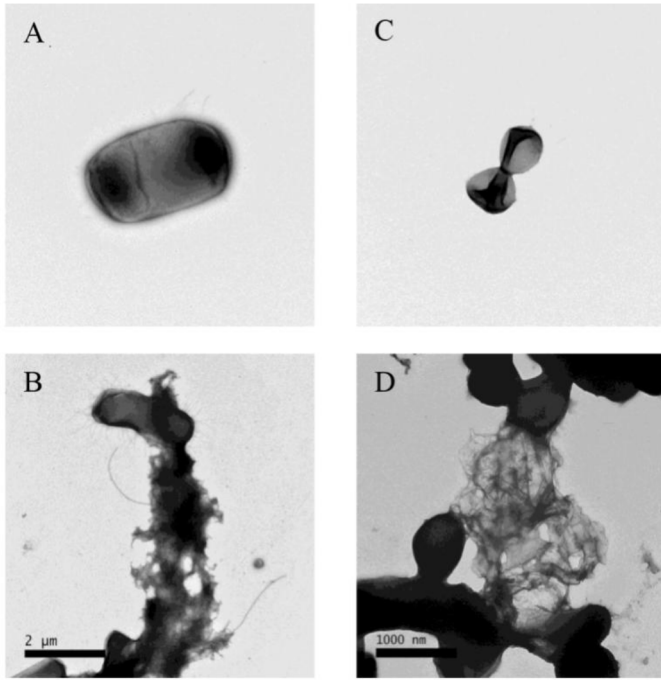


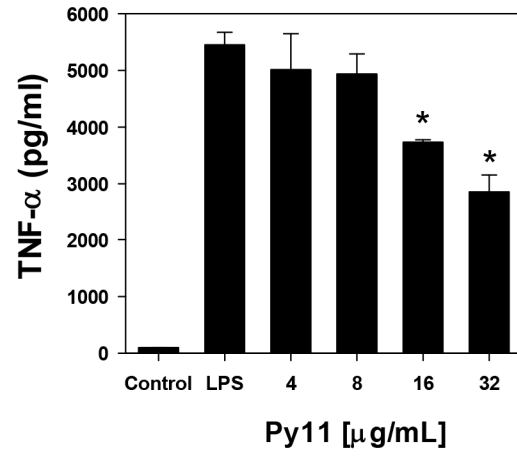
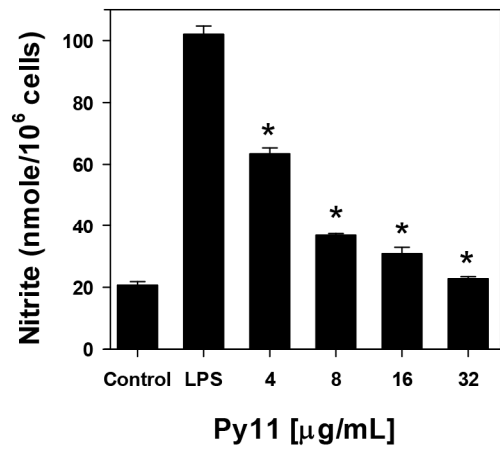


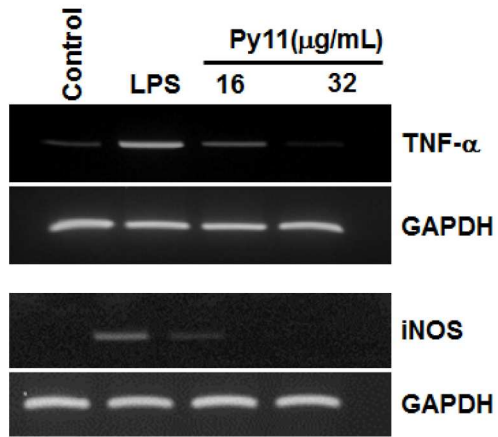












- Synthesis of Fmoc-pyrazole amino acids for the first time
- Synthesis of Pyrazole-arginine based ultra short peptidomimetics using solid phase peptide synthesis
- Ultra short peptidomimetics showed broad-spectrum of antimicrobial activity including MRSA, VREF, and MDRPA
- Ultra short peptidomimetics also showed potent anti-biofilm activity.
- Detailed mechanistic studies including inner membrane permeability, outer membrane permeability, membrane depolarization, and TEM images were performed efficiently.